N70-20414

AN ANALYTICAL AND EXPERIMENTAL STUDY
OF HEAT TRANSFER IN A SIMULATED
MARTIAN ATMOSPHERE

Final Report

by

S. H. Chue, N. Hanus, E. R. F. Winter

AN ANALYTICAL AND EXPERIMENTAL STUDY OF HEAT TRANSFER

IN A SIMULATED MARTIAN ATMOSPHERE

Final Report

Submitted by

Heat Transfer Laboratory
School of Mechanical Engineering
Purdue University
Lafayette, Indiana

to

NATIONAL AERONAUTICS AND SPACE ADMINISTRATION
Jet Propulsion Laboratory
Thermal Control Division
Pasadena, California

Period Covered: November 1, 1968 - October 15, 1969

Principal Investigator: E. R. F. Winter

Contracting Officer's Representative: Donald Ting

Contract Number: 952374   (sub NASA)

Authors: S. H. Chue
           N. Hanus
           E. R. F. Winter

October 1969

ACKNOWLEDGMENT

The authors would like to express their sincere appreciation to Dr. E. R. G. Eckert of the University of Minnesota for critically reviewing the final manuscript and offering many helpf. suggestions.

Special thanks are also due to Jake Bradac, Research Service Co., 985 Englewood Dr. in Minneapolis for helping in the design and the skillful construction of the experimental equipment, and to Bud Goggia of the Jet Propulsion Laboratory for his patient assistance in conducting the experimental portion of this investigation.

TABLE OF CONTENTS

LIST OF TABLES

LIST OF FIGURES

NOMENCLATURE

a	thermal diffisuvity
A	surface area
c_f	skin friction coefficient
c_v	specific heat at constant volume
c_p	specific heat at constant pressure
C_v	molar heat capacity at constant volume
C_p	molar heat capacity at constant pressure
D	diameter of cylinder or sphere
E	energy flux
h	heat transfer coefficient; also enthalpy
k	thermal conductivity of a gas
k'	monatomic or translational thermal conductivity of a polyatomic gas
k"	"internal" thermal conductivity of a polyatomic gas
L	characteristic dimension
M	molecular weight
p	pressure or normal momentum flux
q_i	heat input
q_ℓ	heat losses
q_w''	wall heat flux
Q	heat flow rate

r   recovery factor

r'   modified recovery factor

R   universal gas constant

S   speed ratio

T   temperature

T_c critical temperature

$T_r = \dfrac{T}{T_c}$ reduced temperature

u   streamwise velocity component

v   lateral velocity component; specific volume

x   streamwise distance coordinate

y   lateral distance coordinate

Greek symbols

α accommodation coefficient

β denotes viscosity or thermal conductivity
in Keyes' correlation

γ specific heat ratio

δ boundary layer thickness

ε eddy diffisivity: ε_m, of momentum; ε_h, of
heat; also denotes depth of potential
well or the maximum energy of attraction
between a pair of molecules

k Boltzmann's constant

λ mean free path

μ dynamic viscosity

ρ fluid density

σ collision diameter or reflection coefficient

τ tangential momentum flux

$\Omega^{(l,s)*}$ collision integral involving two molecules

Subscripts

aw   adiabatic wall value

exp   experimental value

i   values of the incident stream

mix   mixture

0   at zero pressure; at standard atmospheric conditions; and also denotes gas properties at the wall in slip flow

s   surface value

r   values of the reflected stream, reference value

w   wall value

$(\bar{\ })$ mean value

∞ free stream value

θ local circumferential value at position making an angle θ with the free stream

Dimensionless Numbers

Kn   Knudsen number

M   Mach number

Nu   Nusselt number

Pr   Prandtl number

Re   Reynolds number

St   Stanton number

St' modified Stanton number

I. INTRODUCTION

During the coming space flights to Mars, thermal design and thermal control will be essential to the success of the mission. The Martian surface lander could conceivably be exposed to ambient temperatures from -180°F to 100°F, and wind velocities up to 250 fps. The surface atmospheric pressure has been estimated in the neighborhood of 6 millibars and carbon dioxide is believed to be the major constituent present. The low pressure existing on the Martian surface lends itself to speculations as to the validity of continuum flow heat transfer correlations as well as the manner in which the transport properties vary under such conditions.

Before an analysis could be performed the above speculations must be cleared up, though unfortunately still not in an absolutely positive manner in one respect. It is shown that the experimental results of Johnston et al.*, usually cited to support the argument that the transport properties are functions of pressure below about 0.1 atm (or approximately 100 millibars), could be used as the basis for a tentative flow regime

---

* See Section 2.5

classification. The agreement of this classification scheme with other schemes proposed on direct experimental basis, e.g. those of Schaaf and Chambre** and Stalder, Goodwin and Creager**, might serve to indicate that these data had been previously misinterpreted. On this basis it is heuristically concluded that the bulk transport properties remain at values predicted by the kinetic theory while low pressure phenomenon due to slight rarefaction could be adequately accounted for by classical slip flow analysis.

The flow regime criterion indicates the occurrence of continuum flow over bodies having sizes of practical importance on the Martian surface. Only laminar flow is expected to exist since the Reynolds numbers are small as a result of low gas densities.

Measurements of forced convection heat transfer from simply shaped objects in a simulated Martian atmosphere were performed to further evaluate the reliability of the established solutions and correlations when used under reduced pressures. These experiments were conducted in a low density wind tunnel. Average film heat transfer coefficients were measured for a flat plate and a cylinder under various pressures and wind velocities in gas mixtures supposedly present in the Martian atmosphere. The models were electrically heated and

---

** See Section 3.4

fully instrumented so that radiation and conduction losses could be accounted for. The steady state power input was monitored for computing these coefficients.

Transport property values for calculating the dimensionless parameters were determined using the Chapman-Enskog theory. Free stream properties were used for calculating the heat transfer coefficients for the flat plate; while properties evaluated at the film temperature were employed for calculating the overall heat transfer coefficients for the cylinder, as suggested by the originators of the correlations. A maximum deviation of 10 percent was found between the experimental data and the values computed from the Pohlhausen solution for the flat plate and the correlations for the cylinder.

In keeping with common practice, two systems of units will be used in this report. The cgs system is used for the transport and thermal properties while the British Engineering system is used for the heat transfer coefficient and several other related parameters.

II. SURVEY OF THERMAL AND TRANSPORT PROPERTIES
OF WORKING FLUIDS

The present literature survey on thermal and trans-
port properties has been conducted within the scope of
the present investigation. Thus, the objective is not
to produce an extensive review of what has been done in
these fields. Only interpolation, extrapolation and
mixing methods which could be used with relative ease
have been included. The relative accuracy of the various
methods are compared, so that a reasonable choice can be
made by the user.

2.1 Theoretical Predictions of Transport Properties

2.1.1 Single Component Systems

2.1.1.1 Viscosity

Theoretical calculations of the viscosity of gases
from kinetic theory have so far met only with limited
success in spite of the amount of effort in that direc-
tion. This is because the calculation of viscosity must
make use of a molecular model for the gas which requires
that certain potential parameters be known. Thus far,
these potential parameters cannot be calculated from

first principles (e.g. from quantum mechanical methods) except for a very few simple cases. For all practical purposes, these potential parameters are obtained by fitting an assumed functional form of the potential function to the experimental data. As it turns out, the most reliable potential parameters known at the present are obtained from none but the viscosity data themselves.

Other complications arise from the fact that for reasons of simplicity the potential functions used in transport property computations are spherically symmetric, such as the Lennard-Jones potential which is by far the most widely used. In reality many molecular species do not have this form of symmetry. Strictly speaking, only monatomic gases have truly spherically symmetric potentials. Potential functions of molecules having an appreciable dipole-moment, the so-called polar molecules, are clearly angular dependent. Even non-polar species, such as carbon dioxide, may deviate substantially from ideal spherical behavior. In the case of carbon dioxide, the deviation is due to molecular complexity, as the carbon dioxide molecule possesses a permanent quadrupole structure.

Another difficulty in using theoretical relations for computing the transport properties lies in the fact that the potential parameters are not universal constants. Keyes [8] has clearly demonstrated this for the

Lennard-Jones potential. His results are reproduced in Table 2.1, just to give an idea of the variations expected even when the data used overlap each other. The Lennard-Jones potential has only two adjustable parameters, σ and ϵ/κ, (these will be defined later when the theoretical calculations are discussed in detail) and therefore requires only two experimental readings at two different temperatures to completely specify them. The trend, which can easily be verified by comparing compilations of these parameters by different authors, is that as σ increases ϵ/κ decreases. However, the relationship governing the variation of σ and ϵ/κ is not known, and all that can be done is to hope that different pairs of values quoted by different authors would predict transport values within a reasonable deviation from the true values. A comparison of the potential parameters for polar gases determined from the averaged Stockmeyer polar potential and the non-polar Lennard-Jones potential, as given in page 267 of reference [13] also illustrates a similar trend of variations between σ and ϵ/κ. Furthermore, the actual numerical values given by the two potential functions are not vastly different from each other. Thus, even for polar gases, there is no advantage in using other more complicated potential functions.

Table 2.1 Values of σ and ϵ/κ Derived from Smoothed
Viscosity Data of CO_2 at Various Temperatures,
from reference |8|.

$\sigma \times 10^8$	ϵ/κ	Temperatures at which Data were Taken
3.955	196.1	273, 373
3.938	202.8	373, 473
3.909	212.2	473, 573
3.874	224.8	573, 673
3.850	235.4	673, 773

The Chapman-Enskog theory to be discussed below is
based on the classical particle-particle collision model,
and includes no quantum effects on the particle behavior.
It has been shown, see reference [6] Chapter 10, that
these results require modification in the temperature
range below 100 K. This is outside the temperature range
of the present investigation, which lies roughly between
170 to 320 K.

Estimation of Gas Viscosity. Theoretical models
are undoubtedly welcome for interpolating or extrapolat-
ing beyond the temperature range of the existing experi-
mental data. Though various empirical correlations can
profitably be used for interpolation, their validity
in extrapolation especially far beyond the range of
experimental data is often doubtful. The only theoretical

method discussed here is that based on the Chapman-Enskog theory of low density gases.

In the first approximation the Chapman-Enskog theory gives the following expression for the viscosity of a pure dilute gas:

$$\mu \times 10^5 = 2.6693 \frac{\sqrt{MT}}{\sigma^2 \, \Omega^{(2,2)*}}$$

where

μ = viscosity in poise or g/cm-s

M = molecular weight

T = absolute temperature, in K

σ = collision diameter, in Å

and $\Omega^{(2,2)*}$ = collision integral involving two molecules

The collision integral is a slowly varying function of the dimensionless temperature $\kappa T/\epsilon$, in which κ is the Boltzmann constant (1.38×10^{-16} erg/K) and ϵ represents the depth of the potential "well" or the maximum energy of attraction between a pair of molecules. The two parameters σ and ϵ are related through the Lennard-Jones potential

$$\phi(v) = 4\epsilon \left[\left(\frac{\sigma}{r} \right)^{12} - \left(\frac{\sigma}{r} \right)^{6} \right]$$

hence, they are commonly referred to as potential parameters. Selected values of σ and ϵ/κ, for various gases related to this particular study, are given in Table 2.2. Values from different sources are quoted, and it should

Table 2.2   Constants for Transport Property Calculations

Gas	Molecular Weight	σ, Å	ϵ/κ, K	Expt. Temp. Range, K
Argon	39.94	3.421^a 3.418^b 3.54^c	119.5^a $124.^b$ $79.^c$	190-1850
CO	44.01	3.952^a 3.996^b 3.94^c	$200.^a$ $190.^b$ $195.^c$	270-1680
N	28.02	3.681^a 3.681^b 3.80^c	91.5^a 91.5^b $71.^c$	130-1700
Air	28.97	3.689^a 3.617^b 3.7^c	84^a 97^b 79^c	190-1850

[a]   from reference [2]

[b]   from reference [6]

[c]   from reference [13]

be noted that the data trend reported earlier holds for most cases. Also to be noted is the extent of deviation in these values. In most instances, the temperature range of the data is not reported. It is expected that the wider the temperature range of the experimental data the more reliably can the parameters be established, and the more reliable is their use for extrapolation. More extensive tabulations of these parameters are widely quoted in the literature, and will not be repeated here.

Note that the kinetic theory model predicts that the viscosity of a gas should be independent of pressure.

This generally agrees well with experimental data up to about 10 atmospheres. At higher pressures, as the kinetic theory assumptions become poorer and poorer, the viscosity increases rapidly with pressure, especially at low temperatures. Since this is outside the scope of the present investigation, this so-called "dense-gas correction" will not be pursued further. On the other hand, at pressures below 0.1 atmosphere, the apparent viscosity observed in laboratory size viscosimeters decreases with decreasing pressure [7]. However, this decrease does not invalidate the kinetic theory prediction and can be attributed to the effect of slip of the molecules on the surface. Because of their small size, slip occurs much earlier in viscosimeters than in most applications. As slip is essentially a boundary phenomenon, the bulk viscosity of the fluid is expected to remain unchanged at its nominal value. It probably will not be until the incipience of near free molecule flow that the bulk viscosity becomes significantly different from the nominal value. Under extremely rarefied conditions, the ordinary concept of viscosity looses its significance since now there is no velocity gradient in the gas.

Viscosity is not influenced by the internal degrees of freedom of the molecules since the momentum exchange mainly concerns the translational kinetic energy. Thus,

the Chapman-Enskog formula has been found to hold remarkably well for polyatomic gases.

To facilitate ease of reference, the collision integral $\Omega^{(2,2)*}$ has been reproduced from reference [6]. This is given in Table 2.3.

2.1.1.2 Thermal Conductivity

Introduction. Much said in the introduction to the preceding section on Viscosity is true also for the thermal conductivity. In addition, however, the situation is further complicated by the fact that energy can also be carried in the internal degrees of freedom of polyatomic molecules.

Estimation of Thermal Conductivity of Gases at Low Densities. The Chapman-Enskog formula for the thermal conductivity of a monatomic gas at low density, in first approximation, is

$$k' \times 10^4 = 1.9891 \frac{\sqrt{T/M}}{\sigma^2 \, \Omega^{(2,2)*}}$$

where   k = monatomic or translational thermal conductivity, in cal/cm-s-K

and other symbols are the same as defined for viscosity. The same potential parameters as tabulated in Table 2.2 are used for calculating k'.

An important result, predicted by rigorous kinetic theory relating μ and k' is as follows:

Table 2.3 The Collision Integral $\Omega^{(2,2)*}$ for the
Lennard-Jones (6-12) Potential, from Reference |6|

$\dfrac{\kappa T}{\varepsilon}$	$\Omega^{(2,2)*}$	$\dfrac{\kappa T}{\varepsilon}$	$\Omega^{(2,2)*}$
0.30	2.785	2.7	1.069
0.35	2.628	2.8	1.058
0.40	2.492	2.9	1.048
0.45	2.368	3.0	1.039
0.50	2.257	3.1	1.030
0.55	2.156	3.2	1.022
0.60	2.065	3.3	1.014
0.65	1.982	3.4	1.007
0.70	1.908	3.5	0.9999
0.75	1.841	3.6	0.9932
0.80	1.780	3.7	0.9870
0.85	1.725	3.8	0.9811
0.90	1.675	3.9	0.9755
0.95	1.629	4.0	0.9700
1.00	1.587	4.1	0.9649
1.05	1.549	4.2	0.9600
1.10	1.514	4.3	0.9553
1.15	1.482	4.4	0.9507
1.20	1.452	4.5	0.9464
1.25	1.424	4.6	0.9422
1.30	1.399	4.7	0.9382
1.35	1.375	4.8	0.9343
1.40	1.353	4.9	0.9305
1.45	1.333	5	0.9269
1.50	1.314	6	0.8963
1.55	1.296	7	0.8727
1.60	1.279	8	0.8538
1.65	1.264	9	0.8379
1.70	1.248	10	0.8242
1.75	1.234	20	0.7432
1.80	1.221	30	0.7005
1.85	1.209	40	0.6718
1.90	1.197	50	0.6504
1.95	1.186	60	0.6335
2.90	1.175	70	0.6194
2.10	1.156	80	0.6076
2.20	1.138	90	0.5973
2.30	1.122	100	0.5882
2.40	1.107	200	0.5320
2.50	1.093	300	0.5016
2.60	1.081	400	0.4811

$$k' = \frac{15}{4} \frac{R}{M} \mu$$

where R = universal gas constant (1.987 cal/mole-K).

In polyatomic gases additional heat is conducted by means of the internal degrees of freedom and a correction to the monatomic value is necessary to predict the thermal conductivity of polyatomic gases.

Various corrections have been proposed. Only two simple practical correction procedures will be discussed below. The first method is due to Eucken, which can be expressed in any of the following forms:

$$k = \left(\frac{C_p}{R} + \frac{5}{4} \right) R \frac{\mu}{M}$$

$$Pr = \frac{1}{1 + 1.25 \ R/C_p}$$

or

$$\frac{k}{k'} = \frac{1}{3} + \frac{4}{15} \frac{C_p}{R}$$

The other is a so-called Eucken-type correction due to Hirschfelder [5], which also can be expressed in similar forms:

$$k = \left(1.328 \frac{C_p}{R} + 0.431 \right) R \frac{\mu}{M}$$

$$Pr = \frac{0.753}{1 + 0.325 \ R/C_p}$$

or

$$\frac{k}{k'} = 0.115 + 0.354 \frac{C_p}{R}$$

Note that these corrections actually allow the thermal conductivity to be computed from knowledge of the viscosity alone. The modified Eucken correction of Hirschfelder had been put onto a firm theoretical basis by Mason and Monchick [9], who obtained this as a first approximation to their rigorous theory. At high temperatures the elaborate theory differs little from the simple modified Eucken correction. However, at low temperatures the rigorous theory leads to better agreement with experimental data. For practical applications, the rigorous theory is rather cumbersome. Thus, based on experimental observations, the procedure below is recommended. For temperatures above room temperature, the Hirschfelder equations are to be used, whereas at room temperature and below, the Eucken correction is to be used:* to be more definitive, we may choose T = 40 C as the dividing temperature.

Values of C_p/R required for making the correction can be obtained from reference [4].

The Eucken correction can lead to errors in k on the order of 10%. For the temperature of interest, the Hirschfelder modification is expected to be even poorer.

If such errors are unacceptable, the Bromley correction can be used. This is discussed in detail in

---

* Correction procedure derived from the following expression given in Reference [9]: "At room temperatures and below, the modified expression is usually poorer than the simple Eucken correction..."

reference [11]. As the gas of interest, mainly CO_2 and N_2, have linear molecules, only the part related to such molecules is given below:

$$k = \left[1.32\ C_V + 3.40 - \frac{0.70}{T_r}\right] \frac{\mu}{M}$$

where k = thermal conductivity at low pressure,

in cal/(s)(cm)(K)

μ = viscosity, in poises

C_V = molar heat capacity at constant volume,

in cal/(g-mol)(K)

T_r = reduced temperature, T/T_c

T_c = critical temperature

and M = molecular weight

This relation is not too cumbersome to use. The required critical temperatures of CO_2 and N_2 are given below.

	CO_2	N_2	Air
T_c,K	304.2	126.2	132.0

2.1.2 Multicomponent Systems

Various mixing rules have been proposed for evaluating the transport properties of a gaseous mixture. However, many of these are restricted to binary mixtures only and their extension to systems having more than two components becomes almost prohibitively involved. Thus, in the present review, only those methods of reasonable

complexity and involving parameters that are readily available are reported.

2.1.2.1 Mixing Rule for Viscosity

The mixing rule for viscosity given below is due to Wilke [14]

$$\mu_{mix} = \sum_{i=1}^{n} \frac{X_i \mu_i}{\sum_{j=1}^{n} X_j \phi_{ij}}$$

where
$$\phi_{ij} = \frac{1}{8} \left[1 + \frac{M_i}{M_j} \right]^{-\frac{1}{2}} \left[1 + \left(\frac{\mu_i}{\mu_j} \right)^{\frac{1}{2}} \left(\frac{M_j}{M_i} \right)^{\frac{1}{4}} \right]^2$$

in which n = number of species in the mixture

X_i, X_j = mole fractions of species i and j

μ_i, μ_j = viscosities of species i and j at system pressure and temperature

M_i, M_j = molecular weights of species i and j

This method has been found to predict values of μ_{mix} within an average deviation of about 2% of the measured values.

A useful relation for computing the ϕ_{ij} values is

$$\phi_{ji} = \phi_{ij} \left(\frac{\mu_j}{\mu_i} \right) \left(\frac{M_i}{M_j} \right)$$

2.1.2.2 Mixing Rules for Thermal Conductivity

The thermal conductivity of gas mixtures at low densities may be estimated by the Wilke Method

$$k_{mix} = \sum_{i=1}^{n} \frac{x_i k_i}{\sum_{j=1}^{n} x_j \, \Phi_{ij}}$$

where
$$\Phi_{ij} = \frac{1}{8} \left[1 + \frac{M_i}{M_j}\right]^{-\frac{1}{2}} \left[1 + \left(\frac{\mu_i}{\mu_j}\right)^{\frac{1}{2}} \left(\frac{M_j}{M_i}\right)^{\frac{1}{4}}\right]^2$$

$$= \frac{1}{8} \left[1 + \frac{M_i}{M_j}\right]^{-\frac{1}{2}} \left[1 + \left(\frac{k_i'}{k_j'}\right)^{\frac{1}{2}} \left(\frac{M_i}{M_j}\right)^{\frac{1}{4}}\right]^2$$

in which

k_i', k_j' = monatomic conductivity of species i and

j at system pressure and temperature.

others are as defined above.

Note that the vi.cosity ratio or the monatomic conductivity ratio of the gas components are being used in computing the function Φ_{ij}.

This method is reported to predict values of k_{mix} with an average deviation of a..out 4% of the measured values for mixtures of non-polar polyatomic gases, including CH_4, O_2, N_2, C_2H_2 and CO.

The accuracy of the predictions can be improved by a modified form of the Wilke formula, which was derived by Mason and Saxena [10] from rigorous kinetic theory by means of well-defined approximations. Agreement is reported to be nearly as good as obtained with the full rigorous theory. This is

$$k_{mix} = \sum_{i=1}^{n} \frac{k_i}{1 + 1.065 \sum_{\substack{j=1 \\ j \neq i}}^{n} \frac{x_j}{x_i} \phi_{ij}'}$$

The ϕ_{ij} functions used here are the same as those used with the Wilke formula.

In both the above methods, the viscosity data should be used when available. If these are unavailable, k' values can be obtained from measured component k values by use of the Eucken-type factor.

$$k' = k/E$$

The relations used for computing E depend on the temperature range.

An extremely simple mixing rule applicable to non-polar gases is due to Brokaw [1]. This is

$$k_{mix} = 0.5\left(k_{sm} + k_{rm}\right)$$

where k_{sm} and k_{rm} are the conductivities based on simple and reciprocal mixing

$$k_{sm} = \sum x_i k_i$$

and

$$\frac{1}{k_{rm}} = \sum \frac{x_i}{k_i}$$

The accuracy is generally poorer than Wilke's formula.

A more satisfactory method involves the division of the thermal conductivity of the mixture of polyatomic gases into two portions [2]:

$$k_{mix} = k'_{mix} + k''_{mix}$$

Here k' represents the monatomic conductivity, as before, whereas k" represents the "internal" conductivity.

The formula used for computing k'_{mix} is given as

$$k'_{mix} = \sum_{i=1}^{n} \frac{k'_i}{1 + \sum_{\substack{j=1 \\ j \neq i}}^{n} \Psi_{ij} \frac{x_j}{x_i}}$$

where $\Psi_{ij} = \Phi_{ij} \left[1 + 2.41 \frac{\left(M_i - M_j\right)\left(M_i - 0.142 M_j\right)}{\left(M_i + M_j\right)^2} \right]$

Here the Φ_{ij} functions are the same as defined previously.

This formula of course can be used for computing k'_{mix} of a monatomic gaseous mixture, though such cases seldom arise in practice. The accuracy seems to be slightly better than the Mason-Saxena method, which is equivalent to writing

$$\Psi_{ij} = 1.065 \ \Phi_{ij}$$

The formula for computing k''_{mix} is the same as the Wilke formula, i.e.

$$k''_{mix} = \sum_{i=1}^{n} \frac{k''_i}{1 + \sum_{\substack{j=1 \\ j \neq i}}^{n} \frac{X_j}{X_i} \phi_{ij}}$$

where k''_i are the internal conductivities of the pure gaseous components. If experimental conductivities of each gas are known, then the k'' values are best obtained as the difference between experimental and monatomic conductivities computed with the Chapman-Enskog theory. If not, k has to be obtained by extrapolation using the same formula.

2.2 Experimental Correlation of Transport Properties of Pure Gases

Interpolation of transport properties by means of the Chapman-Enskog formula is a rather complicated procedure. For this purpose, some empirical correlations would no doubt reduce a substantial amount of computation time. One further advantage offered by the existing correlations is that a single equation, of the three-constant Sutherland type, has been found to correlate successively both the viscosity and thermal conductivity data for a wide variety of gases, including highly polar gases such as steam. This equation is of the form

$$10^5 \beta_0 = \frac{AT}{1 + \frac{B}{T} 10^{C/T}}$$

where β_0 = viscosity, in poise; or thermal conduc-
tivity, in cal/cm-s-K, at zero pressure.

A,B,C = appropriate constants

T = absolute temperature (K)

The values of the constants A, B, and C are widely
scattered in the literature. For this reason, they are
tabulated for all the gases which have been come across,
in the course of this work, and not merely for the three
gases of interest. These are given in Tables 2.4 and
2.5. In all cases, the constants that are believed to
be most up to date are used.

These correlation formulas are valid only at low
pressures. The pressure effects are not significant
within the scope of the present investigation and they
are not reported.

In general, correlation formulas are not used for
gaseous mixtures since even a binary mixture could have
an infinite number of compositions. Any of the mixing
rules listed earlier can be used to find the transport
properties of the required mixture.

All the correlations presented in Tables 2.4 and
2.5 were taken from various publications of Keyes in
the Trans. ASME during the period 1950 through 1955.

Table 2.4   Correlation Constants for Viscosities
at Low Pressure

Gases	A	B	C	Temp. Range, K
A	2.173	218.4	14	55- 273
	1.910	136.6	0	180-1873
He	0.848	1.593	0	1.64- 20
	$\log(10^5\mu) = 1.722 + 0.6268 \log T$			20- 140
	1.805	251.0	50	140- 373
Ne	1.975	37.7	0	80- 160
	2.356	98.9	18	169- 370
	$\log(10^5\mu) = -0.0705 + 0.636 \log T$			370-1100
H_2	0.623	70.8	17.7	90- 551
O_2	1.739	142.0	5.0	90- 373
N_2	1.418	116.4	5.0	90-1695
Air	1.488	122.1	5.0	90-1845
CO	1.495	143.2	6.0	80- 549
CO_2	1.554	246.0	3.0	198-1686
H_2O	1.501	446.8	0	373- 873

Table 2.5   Correlation Constants for Thermal
Conductivities at Low Pressure

Gases	A	B	C	Temp. Range, K
A	0.384	178.8	8.0	90-620
He	2.35	43.5	10	15-375
Kr	0.225	240.	12	130-580
Ne	0.83	70.5	10	90-579
Xe	0.154	378.	25	155-273
H_2	3.76	166.	10	90-595
O_2	0.606	206.2	6	86-373
N_2	0.615	235.5	12	90-823
Air	0.632	245.	12	90-584
CO	0.586	218.0	7.8	90-375
CO_2	3.333	4433	10	190-592
H_2O	1.546	1737.3	12	373-823

2.3 Thermodynamic Properties of Pure Gases

The pertinent thermodynamic properties required in the prediction of heat transfer are the specific heat at constant pressure and the density

Empirical equations have been established for specific and molar heats at various pressures and temperatures. Such a collection of equations has been given, for instance, in "Empirical Specific Heat Equation Based upon Spectroscopic Data," by R. L. Sweigert and M. W. Beardsley, Georgia School of Technology Engineering Experimental Station, Bulletin No. 2, 1938, which has been reproduced in part in [3, 12]. To be able to interpolate between these pressures, the following thermodynamic relation has to be used

$$c_p - c_{p_r} = - \left[\int_{p_r}^{p} T \left(\frac{\partial^2 v}{\partial T^2} \right)_p dp \right]_T$$

This requires the availability of the p-v-T data in the range considered. However, the presence of p-v-T data alone is sufficient for deriving the specific heat at all other pressures if the values at a common reference pressure, say at zero pressure, are known. The experimental values may then be used merely as a check of the numerical process. The procedure for obtaining the values at any pressure other than the reference value is therefore very cumbersome. It is best obtained from

tabulated data, such as from reference |4|. Owing to the low pressure existing in the Martian atmosphere, the specific heat values would not deviate very much from the zero pressure reference values.

The density ratio, ρ/ρ_0, where ρ_0 is the density at standard conditions (273.16 K and 1 atm) can be predicted with sufficient accuracy with the ideal gas relation:

$$\frac{\rho}{\rho_0} = \frac{P}{P_0} \frac{T_0}{T}$$

From reference |4|, the error is seen to be within 1 part in ten thousand down to temperatures of about 200 K. The value for ρ_0 for the working gases are quoted below

ρ_0	Air	Argon	CO_2	N_2
g/cm³	1.2930 ×10⁻³	1.78377×10⁻³	1.9770×10⁻³	1.25046×10⁻³
lb/in³	4.67143×10⁻⁵	6.44432×10⁻⁵	7.1424×10⁻⁵	4.51760×10⁻⁵
lb/ft³	8.07223 10⁻²	0.111358	0.12342	7.80641 10⁻²

2.4 Thermodynamic Properties of Gas Mixtures

Since the densities of the gases under operational conditions are very low relative to the critical density of any of the components, the Gibbs-Dalton law is expected to hold very well. Thus, the various thermodynamic properties of the mixture could be computed from the following relations:

Density
$$\rho_{mix} = \sum_i \rho_i$$

Specific heats

$$c_{p_{mix}} \left(\text{or } c_{v_{mix}}\right) = \sum_i W_i \; c_{p_i} \left(\text{or } c_{v_i}\right)$$

where W_i = mass fraction

Molar specific heats

$$C_{p_{mix}} \left(\text{or } C_{v_{mix}}\right) = \sum_i x_i \; C_{p_i} \left(\text{or } C_{v_i}\right)$$

where x_i = mole or volume fraction

Molecular weight

$$M_{mix} = \sum x_i M_i$$

2.5 Cited References

1. Brokaw, R. S., Ind. Eng. Chem., 47, 1955, p. 2398.

2. Brokaw, R. S., NASA TR R-81, 1961.

3. Hawkins, G. A., Thermodynamics, Wiley, 2nd ed., 1946.

4. Hilsenrath, J., et al., Tables of Thermal Properties of Gases, National Bureau of Standards Circular 564, Issued No. 1955.

5. Hirschfelder, J. O., J. Chem. Phys., 26, 1957, p. 282.

6. Hirschfelder, J. O., Curtiss, C. F. and Bird, R. B., Molecular Theory of Gases and Liquids, Wiley, 2nd Printing, 1964.

7. Johnston, H. L., Mattox, R. W., and Powers, R. W., Viscosities of Air and Nitrogen at Low Pressures, NACA TN 2546, 1951.

8. Keyes, F. G., Trans. ASME, 73, 1951, p. 589-96.

9. Mason, E. A. and Monchick, L. J., Chem. Phys., 36, 1962, p. 1622.

10. Mason, E. A. and Saxena, S. C., Phys. of Fluids, 1, 1958, p. 361-9.

11. Reid, R. C. and Sherwood, T. K., The Properties of Gases and Liquids, McGraw-Hill, 1958.

12. Van Wylen, G. J., Thermodynamics, Wiley, 1959.

13. Westenberg, A. A., Advances in Heat Transfer, Vol. 3 Academic Press, 1966, pp. 253-302.

14. Wilke, C. R., J. Chem. Phys., 18, 1950, p. 517-9.

III. REVIEW OF FORCED CONVECTION HEAT TRANSFER
UNDER REDUCED PRESSURES

The present survey of convective heat transfer
under reduced pressure is divided into three sections.
The first section concerns the classification of the
flow situation into various regimes depending on the
degree of rarefaction. The second gives a review of
the existing solutions in the different regimes. Only
external flow solutions are reported. Solutions obtained
with simplifying assumptions such as those applied spe-
cifically to liquid metals have been excluded, since
these obviously lie outside the scope of the present
investigation. Detailed procedures for obtaining these
solutions are not reported as it is not the purpose of
this survey to repeat unnecessarily any of this material,
which can be obtained either from standard sources or
from the specific references listed in the bibliography.
The last section reports existing solutions and correla-
tions for predicting heat transfer for the special cases
of flow over a flat plate, a cylinder and a sphere.
However, the listing is not meant to be exhaustive. In
the continuum regime, the analogy between fluid friction
and heat transfer has been used extensively, especially

in turbulent flows. Therefore, in this regime, the fluid friction correlations are also reported.

3.1 Flow Regimes

It is well known that the degree of rarefaction of a gas influences the flow and heat transfer characteristics of the gas to a surface. For the purpose of classifaction, we distinguish four different regimes depending on the ratio of the mean free path λ of the gas molecules to the characteristic dimension L of the flow system. This corresponds to ordinary (continuum), slightly rarefied (slip), moderately rarefied (transition) and highly rarefied (free molecule) situations.

The mean free path is related to the viscosity of the gas by the equation

$$\mu = 0.5 \ \rho \bar{u} \lambda \qquad (1)$$

Here, $\bar{u}$ is the average velocity for the molecules having a Maxwellian distribution, given by

$$\bar{u} = \sqrt{\frac{8}{\pi}} \sqrt{RT} = \sqrt{\frac{8}{\pi \gamma}} \ a \qquad (2)$$

where   R = gas constant

γ = ratio of specific heats

a = acoustic velocity at temperature T.

Substitution of Eq. (2) into (1) gives

$$\lambda = 1.255 \ \sqrt{\gamma} \left(\frac{\nu}{a} \right) \qquad (3)$$

which can be put into the following form

$$\lambda \left(\frac{p}{p_0} \right) = \frac{1.255}{\sqrt{gR}} \frac{\mu\sqrt{T}}{p_0 T_0} \tag{4}$$

where the subscript 'o' denotes quantities at standard atmospheric conditions. For air, on substituting the relevant values, Eq. (4) becomes

$$\lambda \left(\frac{p}{p_0} \right) = 3.5865 \times 10^{-7} \left(\frac{\mu}{\mu_0} \right) \sqrt{T}$$

where λ is now in cm and T in centigrade degrees.

The quantity $\lambda \left(\frac{p}{p_0} \right)$ is tabulated in Table 3.1, from which it is seen that at ordinary pressures, the mean free path is truly negligible in comparison with any characteristic length that may occur in gas dynamics and convection problems.

Table 3.1 Mean Free Path for Air

Temperature, K	$\lambda \left(\dfrac{p}{p_0} \right) \times 10^6$, cm.
150	2.63
200	3.92
250	5.28
300	6.68
350	8.10
400	9.55

The parameter used to characterize the flow regimes as defined earlier is usually known as the Knudsen number. Making use of Eq. (3), it can be written as

Continuum Flow

$$\frac{M}{\sqrt{Re}} < 0.01 \qquad \text{for } Re \gg 1$$

$$\frac{M}{Re} < 0.01 \qquad \text{for } Re < 1$$

Slip Flow

$$0.01 < \frac{M}{\sqrt{Re}} < 0.1 \qquad \text{for } Re \gg 1$$

$$0.01 < \frac{M}{Re} < 0.1 \qquad \text{for } Re < 1$$

Transition Flow

$$0.1 < \frac{M}{Re} < 3$$

Free Molecule Flow

$$\frac{M}{Re} > 3$$

However, it should be realized that the above criteria is only approximate as only at low speeds is the mean free path essentially constant over the flow domain and thus the above ratios are well defined. Even under such conditions, the lack of precision in the definition of these boundaries is apparent, since the same order of magnitude is used for the regime boundaries defined by both M/Re and M/√Re. At high speeds, λ is probably to be evaluated at wall conditions--and also δ now depends on M, the local heat transfer conditions, and the position on the body as well as on Re. Thus, care must be exercised in evaluating the Knudsen number criteria with respect to the particular phenomenon of interest.

3.2 Past Investigations

In this section, the different methods employed in solving the problems in each regime are outlined. Past investigations of forced convection heat transfer from bodies immersed in an external stream are summarized.

3.2.1 Continuum Regime

Of all the four flow regimes mentioned in Section 1, this is the most well developed, perhaps because this corresponds to ordinary surrounding conditions. Interest in this has been shown since the time of Newton. To date, the most complete formulation of continuum flow mechanics is found in the Navier-Stokes equations. Even for two-dimensional or axisymmetric flows, the solution of the Navier-Stokes equations is still exceedingly complicated. Thus far very few exact solutions have been obtained and most of these are for very simple flow configurations such that most of the terms in the equations drop out. Even with the help of high speed computers, not many numerical solutions of the Navier-Stokes equations have been reported, as this is still a time consuming and costly matter.

Fortunately, most of the common fluids have very small viscosities and consequently the Reynolds number is very large. Realizing this, Prandtl was able to achieve a far reaching simplification, resulting in the

well-known Boundary Layer equations. For two-dimensional, laminar, external flows, the momentum equations for a fluid having constant properties are

$$\rho \left[\frac{\partial u}{\partial t} + u \frac{\partial u}{\partial x} + v \frac{\partial u}{\partial y} \right] = - \frac{\partial p}{\partial x} + \mu \frac{\partial^2 u}{\partial y^2} \tag{6}$$

and

$$\frac{\partial p}{\partial y} = 0 \tag{7}$$

The problem is completely determined together with the continuity equation, given by

$$\frac{\partial u}{\partial x} + \frac{\partial v}{\partial y} = 0 \tag{8}$$

and the appropriate boundary conditions as well as the external pressure gradient in the streamwise direction. This is so because the pressure ceases to be an unknown quantity under the boundary layer assumptions, being now given by the free stream Bernoulli equation

$$\frac{dp}{dx} + \rho u_\infty \frac{du_\infty}{dx} = 0 \tag{9}$$

The above equations have been extensively investigated for the steady planar situation. There are tabulated in Table 3.2.

Heat transfer between the fluid and the wall occurs when the temperature in the fluid is different from that of the body. In order to predict the heat transfer, we need an additional thermal energy equation. Subject to the same constant property assumption, this is,

Table 3.2

Solutions for Steady Incompressible Planar Flows

Case Treated	Investigator	Reference
Flat plate	Blasius	NACA TM 1256, Z. Math. Phys., $\underline{56}$, 1908, p. 1
wedge flow: $u_1(x) = Cx^m$	Falkner-Skan	Phil. Mag $\underline{12}$, 1931, p. 865 ARC R & M 1314, 1930
	Hartree	Proc. Cambr. Phil. Soc., $\underline{33}$, Part II, 1937, p. 223
Flow with $u_1(x) = u_0 - ax^n$	Howarth	Proc. Roy. Soc., London, A $\underline{164}$, 1938, p. 547
	Tani	J. Phys. Soc., Japan, $\underline{4}$, 1949, pp. 149-154.
Back flow	Stewartson	Proc. Cambr. Phil. Soc., $\underline{50}$, 1954, p. 454.

$$\rho c_p \left[u \frac{\partial T}{\partial x} + v \frac{\partial T}{\partial y} \right] = k \frac{\partial^2 T}{\partial y^2} + \mu \left(\frac{\partial u}{\partial y} \right)^2 \qquad (10)$$

The viscous dissipation term can be important for high Prandtl number fluids even at moderate speeds. For fluids of Prandtl numbers on the order of one, however, the velocity must reach the acoustic speed before this term becomes important. Thus for ordinary situations, this term can be neglected, and Eq. (10) reduces to

$$\rho c_p \left[u\, \frac{\partial T}{\partial x} + v\, \frac{\partial T}{\partial y} \right] = k\, \frac{\partial^2 T}{\partial y^2} \tag{11}$$

The system of equations including heat transfer have also been extensively investigated. These are tabulated in Table 3.3.

When the flow is turbulent, both the Navier-Stokes and the energy equations remain valid if the instantaneous pressure, temperature and velocity components are used. However, a solution in terms of the instantaneous values does not have direct application and moreover, this is beyond the present state of the art. The present procedure is to time average the equations. After some further simplifying assumptions the resulting time-averaged boundary layer equations retain only one double correlation term each. Following Bossinesq, these double correlation terms can be related to the gradients of the mean quantities

$$-\overline{u'v'} = \epsilon_m\, \frac{\partial \overline{u}}{\partial y}$$

$$-\overline{u'T'} = \epsilon_h\, \frac{\partial \overline{T}}{\partial y}$$

Substitution of these relations into the time averaged equations reduces them to forms similar to those of (6) and (11). Only now the terms involving the molecular effects in the momentum and energy equations in laminar flow are replaced by $\frac{\partial}{\partial y}\left[(\mu + \rho\epsilon_m)\frac{\partial u}{\partial y} \right]$ and $\frac{\partial}{\partial y}\left[(k + \rho c_p \epsilon_h)\frac{\partial T}{\partial y} \right]$ respectively. Even though the form of the equations remains essentially unchanged

Table 3.3

Heat Transfer Solutions for Steady, Incompressible Planar Flows

Cases Treated	Investigator	Reference
Flat plate, const. wall temperature	Pohlhausen	ZAMM, 1, 1921, pp. 115-21
Flat plate, variable wall temperature	Rubesin	M.S. Thesis, Univ. of Calif., Berkeley, June, 1947
Flat plate, variable heat flux	Tribus & Klein	ASME Paper No. 55-SA-46, 1955
Flat plate, const. wall temperature, with suction or blowing	Mickley, Ross, Squyers, & Stewart	NACA TN 3208, 1954
	Eckert	Air Force Air Material Command Tech. Rept. 5646, Nov. 1947
	Emmons & Leigh	British ARC CP 157, 1954
Wedge flow, const. wall temperature	Eckert	VDI Forschungsheft 416, 1942
Wedge flow with wall temperature variation given by $T_W-T_s=Dx^\gamma$	Fage & Falkner	British ARC R & M 1408, 1930
	Lighthill	Proc. Roy. Soc., A202, 1950, p. 359
	Levy	JAS, 19, 1952, p. 341
Stagnation point	Squire	reported in book by Goldstein

their solutions become extremely complicated. For the momentum equation alone, over sixty numerical techniques have been reported for its solution, though the myriad of solutions does not all make use of Bossinesq's concept, which is by far the most commonly used. That so many solutions are possible is due to the fact that the turbulent equations have more unknowns than the number of equations. No attempt is made to enumerate all of these solutions. At present, nearly all engineering predictions of heat transfer in turbulent flow are based on the analogy between heat and momentum transfer. Satisfactory results were obtained with the exception of fluids of extremely small Prandtl number.

For flow over a flat plate, an approximate velocity profile based on mixing length or similarity theories has been developed. However, for ease of integration, a 1/7-th power law is often used to represent both the velocity and temperature distributions. Using procedures similar to those in laminar flow, cases for arbitrary wall temperature and heat flux have also been treated [20, 21].

In all the solutions considered up to this point, the effects of the viscous dissipation has been neglected. When this effect is included, the thermal energy equation (10) for laminar flow can be put into the following form when the fluid properties are assumed constant.

$$u \frac{\partial T}{\partial x} + v \frac{\partial T}{\partial y} = \alpha \left[\frac{\partial^2 T}{\partial y^2} + \frac{Pr}{c_p} \left(\frac{\partial u}{\partial y} \right)^2 \right] \tag{12}$$

It is therefore seen that the dissipation effect depends not only on the velocity gradient but also on the Prandtl number. For high Prandtl number fluids this can be important even at moderate velocities and velocity gradients. However, for gases, the Mach number must approach unity before this effect is significant.

Eq. (10) has been solved for an adiabatic flat plate by Pohlhausen [17]. Since the energy equation is linear in T, the general case of a nonadiabatic wall can be obtained by superposing solutions of Eqs. (10) and (11) in such a way that the boundary conditions are satisfied. This results in the statement that the low speed relations can be used if now the heat transfer coefficient is defined in terms of $(T_w - T_{aw})$ instead of $(T_w - T_\infty)$. Thus the problem reduces to that of finding the recovery factor, r, which allows the adiabatic wall temperature T_{aw} to be determined, since these two quantities are related by

$$r = \frac{T_{aw} - T_\infty}{T_{st} - T_\infty} = \frac{T_{aw} - T_\infty}{u_\infty^2 / 2c_p}$$

where T_{st} is the stagnation temperature, defined as the temperature that a gas will attain if brought to rest reversibly and adiabatically.

Turbulent high velocity flow over a flat plate has also been studied [1, 9] and it has been found that the same conclusion applies.

In all the solutions considered so far the effect of variations in fluid properties has been neglected. Such solutions are expected to hold up to low supersonic flows, (M · 2) and modest temperature differences, at sections far away from the leading edge such that the effect of the leading edge shock could be ignored. Schlichting [22] suggested that the effect of variable properties should be taken into account when the temperature difference exceeds 50°C or 90°F.

Now, the system of boundary layer equations is given by

$$\frac{\partial(\rho u)}{\partial x} + \frac{\partial(\rho v)}{\partial y} = 0$$

$$\rho\left(u\ \frac{\partial u}{\partial x} + v\ \frac{\partial u}{\partial y}\right) = -\frac{dp}{dx} + \frac{\partial}{\partial y}\left(\mu\frac{\partial u}{\partial y}\right) \tag{13}$$

$$\rho c_p\left(u\ \frac{\partial T}{\partial x} + v\ \frac{\partial T}{\partial y}\right) = \frac{\partial}{\partial y}\left(k\ \frac{\partial T}{\partial y}\right) + \mu\left(\frac{\partial u}{\partial y}\right)^2$$

Using the Howarth transformation [14]

$$\xi = x, \quad \eta = \int_0^y \frac{\rho}{\rho_\infty}\ dy$$

this system of equations becomes

41

$$\frac{\partial u}{\partial x} + \frac{\partial \bar{v}}{\partial \eta} = 0$$

$$\rho_\infty \left(u \frac{\partial u}{\partial x} + \bar{v} \frac{\partial u}{\partial \eta} \right) = - \frac{\rho_\infty}{\rho} \frac{dp}{dx} + \frac{1}{\rho_\infty} \frac{\partial}{\partial \eta} \left(\mu \rho \frac{\partial u}{\partial \eta} \right) \qquad (14)$$

$$\rho_\infty c_p \left(u \frac{\partial T}{\partial x} + \bar{v} \frac{\partial T}{\partial \eta} \right) = \frac{1}{\rho_\infty} \frac{\partial}{\partial \eta} \left(\frac{\mu \rho c_p}{Pr} \frac{\partial T}{\partial \eta} \right) + \frac{\mu \rho}{\rho_\infty} \left(\frac{\partial u}{\partial \eta} \right)^2$$

where $\qquad \bar{v} = \frac{\rho}{\rho_\infty} \left(v - u \frac{\partial y}{\partial \xi} \right) = - \int_0^\eta \frac{\partial u}{\partial \xi} \, d\eta$

The boundary conditions for this system are identical
with those for the original system if y and v are
replaced by η and $\bar{v}$ respectively.

Hence it can be seen that the assumption of con-
stant $\mu\rho$ and c_p/Pr reduces equation (14) to the same
form as if the flow were incompressible. This therefore
leads to relations for the friction factor and the
Nusselt number identical to the corresponding constant
property solutions. All properties can be evaluated
at the free stream temperature and the viscous effect
can be taken care of by introducing the adiabatic wall
temperature. This analysis illustrates that the property
variations tend to compensate and despite large varia-
tions in a real gas the constant property solutions have
a remarkable range of validity.

Van Driest [26] has reported a more elaborate
analysis of the laminar case by introducing a Sutherland

law variation for μ. The case for turbulent flow has been treated by Deissler and Loeffler [4] using power law variations for μ and k. Despite the temperature dependence of the fluid properties, the constant property recovery factors remains in satisfactory agreement.

The effect of compressibility can be treated in a similar manner as the variable property analysis. Usually for the sake of simplicity, the ideal gas law is used to relate the pressure, density and temperature of the gas. This relation is assumed to hold for Mach numbers below hypersonic speeds, corresponding to $M > 6$; (p. 312 of reference [22]). For $Pr = 1$, the adiabatic wall temperature in compressible flow is identical with that for an incompressible fluid. Emmons and Brainerd [10] have shown that in the case of Prandtl numbers differing from unity the deviations in wall temperatures caused by compressibility effects are very small. Thus the incompressible equation remains valid.

All the solutions reported are for the planar flow configuration. Practical cases undoubtedly involve bodies having arbitrary shapes. Approximate methods have been devised for calculating the heat transfer coefficient for laminar [6, 7, 23] and turbulent [2, 24, 19] flows over a body of revolution with arbitrary shape having

constant wall temperature up to the point of separation.
In the case of the laminar constant-property boundary
layer, Spalding and Pun [25] have carried out an exten-
sive survey of the methods used for calculating heat
transfer from an arbitrary shaped body. A comparison
of the methods was made by applying them to the calcu-
lation of heat transfer from the front half of a
circular cylinder in cross flow. The simple geometrical
shapes such as the cylinder and sphere have been rather
extensively investigated. These are tabulated in Tables
3.4 and 3.5. However, at present analytical solutions
exist only when the flow is laminar, and before separa-
tion occurs.

Though the effects of compressibility and property
variations are discussed separately above, both terms
actually describe the same phenomenon observed in high
speed flows. All turbulent heat transfer solutions
reported so far are based on the integral method.
However, recently many attempts have been made to
predict heat transfer by using the differential equa-
tions. A good collection of numerical methods used
for predicting the isothermal turbulent boundary layer
is given in Volume 1 of the Proceedings of the 1968
AFOSR-IFP-Stanford Conference on Computation of Turb-
ulent Boundary Layers. Extensions of these methods

Table 3.4

Heat Transfer Investigations on Cross Flow Over a Cylinder

Investigator	Reynolds Number Range*	Theo-retical	Experi-mental	Reference
Benke			x	Arch. Wärmen, 19, 1958, p. 287
Churchill & Brier	500<Re<2250		x	Chem. Eng. Progr. Symp. Ser., 17, 51, 1955, p. 57
Comings, Clapp & Taylor	Re>1000		x	Ind. Eng. Chem., 40, 1948, p. 1076
Dienemann		x		ZAMM, 33, 1953, pp. 89-109
Eckert		x		VDI Forschungsheft 416, 1942
Eckert & Soehngen	20<Re<600		x	ASME, 74, 1952, p. 343
Foressling		Exact Solution		NACA TM 1432
Giedt	Re>1000		x	JAS, 18, 1951, p. 725; also ASME, 71, 1949, p. 375
Hilpert	1<Re<400,000		x	Forsl. Gebiete Ingenieurw., 4, 1933, p. 215-24
Krujilin	Re<1000		x	Tech. Phys. USSR, 5, 1938, p. 289
Krujilin		x		Tech. Phys. USSR, 3, 1936, p. 311
Lorisch	Re>1000		x	VDI Forschungsheft 322, 1929
Perkins & Lippert			x	ASME, 84C, 1962, pp. 257-263
Reiher			x	Forsch. Gebiete Ingenieurw., 269, 1925, p. 1
Sauer & Drake		x		JAS, 20, 1953, pp. 175-80
Schmidt & Wenner	4000<Re<450,000		x	NACA TM 1050, 1943
Ulsamer	0.1<Re<10000		x	Forsch. Gebiete Ingenieurw., 5, 1932, p. 94
Zapp	Re>1000		x	M.S. Thesis, Oregon State College, 1950, discussed in Knudsen & Katz, ref. [16]

* Reynolds number is based on diameter of cylinder

Table 3.5
Heat Transfer Investigations on Flow Over a Sphere

Investigator	Reynolds* Number Range	Theo-retical	Experi-mental	Reference
Brown Pitts, Leppert		x	x	ASME, 84C, 1962, pp. 133-40
Carey	44,000<Re<150,000		x	ASME, 75, 1953, p. 483
Drake & Kane		x		General Discussion on Heat Transfer, London, 1951, p. 119; see also Inst. of Engrg. Res. Rept. No. HE-150-74, U. of Calif., Berkeley, Nov. 1950
Froessling		x		NACA TM 1432, 1958
Hughes			x	Phil. Mag. (6), 31, 1916, p. 118
Johnstone, Pigford & Chapin			x	Trans. AIChE, 31, 1941, p. 95
Kramers	10<Re<100,000		x	Physica, 12, 1946, p. 61
Audryashev		x	x	Bull. Acad. Sci. USSR, Sci. Tech., 11, 1949, p. 1620
Lorisch	Re>1000		x	VDI Forschungsheft 322, 1929
Loyzansky & Schwab			x	Central Aero-hydro-dynamic Inst. Rept. 329, USSR, 1935
Ranz			x	Chem. Eng. Prog. 48, 1952, p. 247
Ranz & Marshall			x	Chem. Eng. Prog. 48, 1952, p. 141
Reiher			x	Forsch gebiete Ingenieurw., 269, p. 1, 1925
Tang, Duncan & Schweyer	50<Re<1,000	x	x	NACA TN 2867, 1953
Vyrubov			x	J. Tech. Phys., USSR, 9, 1939, p. 1923.

* Reynolds number is based on diameter of sphere

into heat transfer have been reported by several authors,
e.g., Spalding et al., Cebeci and Smith, and Mellor and
Herring.

3.2.2 Slip Flows

Slip flow is the branch of rarefied gas dynamics
corresponding to only slight rarefaction for which the
departure from continuum gas dynamics is slight. From
the flow regime classification for slip flow given in
Section 1, it is seen that for the ratio M/Re or M/$\sqrt{Re}$
to lie in the given range either M must be large, or Re
must be small, or both. Hence slip flow is usually
dominated by very strong compressibility or viscous
effects. Thus it is to be expected that the boundary
layers in the presence of slip are laminar. They will
often be quite thick and in fact the Reynolds number
may be so low that boundary layer theory is strictly
not applicable. It is also to be expected that inter-
action between the boundary layer and the supersonic
inviscid free stream flow will become important.

The fundamental problem of the correct formulation
of the slip flow phenomenon has not been resolved in a
satisfactory way. It has been argued that some modifi-
cation of the Navier-Stokes equations, such as the
Burnett equations [28] or thirteen moment equations [31]
could account for some of the experimentally observed

phenomena associated with slip flow. However, recent
experimental evidence seems to indicate that the Navier-
Stokes equations, together with velocity and temperature
jump boundary conditions, are not only adequate but
probably even superior to these modified forms.

The slip boundary conditions are [35]

$$u(0) = \frac{2-\sigma}{\sigma} \lambda \left(\frac{\partial u}{\partial y}\right)_0 + \frac{3}{4} \frac{\mu}{\rho T}\left(\frac{\partial T}{\partial x}\right)_0$$

$$T(0) - T_w = \frac{2-\alpha}{\alpha} \frac{2\gamma}{\gamma+1} \frac{\lambda}{Pr}\left(\frac{\partial T}{\partial y}\right)_0$$

Here, the subscript "o" indicates that the parameters
are evaluated for the gas at the wall.

   σ = reflection coefficient, representing the

      fraction of diffusely reflected molecules

   α = accommodation coefficient

The definition of these coefficients in terms of the
physical fluxes at the wall will be given in Section
3.2.4.

There have been some disagreements on the tempera-
ture jump condition for polyatomic gases. However, for
macroscopic considerations, these do not represent any
serious obstacle since they only correspond to different
ent macroscopically determined values for o and α. At
present it seems that the most serious obstacle against
accurate prediction of slip flow is the lack of confi-
dence in the experimentally measured accomodation

coefficients. Devienne [30] has suggested that nearly all the measurements should be taken up again, with complete specification of all relevant factors--and he has listed no less than thirteen of them!

Closed form solutions have been obtained for the flat plate by neglecting the viscous dissipation term and applying the Oseen approximation to the boundary layer equation [29, 36]. The Oseen simplification that the velocity deviates from the free stream value by a small amount should become progressively better as the slip increases. However, it should also be realized that the Oseen solution gives an incorrect limit in the continuum regime, hence, the solutions so obtained would not be reliable even in the near-continuum region. Solution for forced convection heat transfer in slip flow from a normal horizontal cylinder has been obtained by Sauer and Drake [33] using several simplifying assumptions. The corresponding solution for a sphere was reported by Drake and Kane [29].

In general, the effect of slip is to decrease the heat transfer and skin friction from the corresponding continuum values. In this respect, it should be noted that the solution reported by Schaaf for the flat plate gives Nusselt numbers higher than the continuum solution. This seems to contradict the general trend established by other solutions, both in internal and external situations.

3.2.4 Free Molecule Flow

This regime corresponds to that of extreme rarefaction. The basic assumption is that intermolecular collisions can be neglected. Consequently, it is valid to neglect the effect of the reemitted particles on the incident stream. Hence, the incident flow is entirely undisturbed by the presence of the body, even in supersonic flow. Therefore, no shock waves are expected to form in the vicinity of the object.

Contrary to the transition flow regime, the fundamental characteristics of free molecule flow are sufficiently simple so that theoretical analysis may be made; this is especially so for convex surfaces because now all incident molecules must originate in the free stream. These calculations have generally been verified experimentally. In calculating the flux of momentum or energy it is assumed that the approaching molecules are in Maxwellian equilibrium with respect to the macroscopic velocity.

As expected, the specification of the mechanics of collision of the molecules with the wall is given in terms of the accommodation coefficient α and the reflection coefficient σ, which have been encountered before in describing the slip flow boundary conditions. These coefficients are defined as follows:

$$\alpha = \frac{E_i - E_r}{E_i - E_w}$$

where E = energy flux (energy per unit area per second)
and the subscripts i, r, and w refer to the incident,
reflected and wall conditions, respectively. In some
cases it is convenient to replace E by T in the above
definition. This assumes that the energies are propor-
tional to the temperatures. However, this condition is
only valid for monatomic molecules since only the energy
of translation is directly proportional to the absolute
temperature.

and $$\sigma = \frac{\tau_i - \tau_r}{\tau_i - \tau_w} \qquad (\tau_w = 0)$$

$$\sigma' = \frac{p_i - p_r}{p_i - p_w}$$

where τ = tangential momentum flux

p = normal momentum flux.

The concept of describing the overall interaction in
terms of these coefficients is useful only if they are
reasonably constant for a given gas-surface combination.
This appears to be the case for technical surfaces, at
least for α and σ. The experiments of Stickney [45]
indicated that σ' might be sensitive to the inclination
of the velocity vector to the surface.

Heat transfer and friction predictions in free molecule flow have been obtained for flow over a flat plate [43], a cylinder in cross-flow [44] and over a sphere [41]. A very detailed summary of these situations together with a method for constructing solutions for more complicated body configurations out of these simple geometrical shapes were reported by Oppenheim [39].

3.3 Solutions and Correlations for Prediction of Heat Transfer

In this section only closed form solutions and correlations will be listed. The space available does not permit the reproduction of all tabular solutions.

3.3.1 Laminar Continuum Flow

3.3.1.1 Flat Plate

The skin friction coefficient is given by the Blasius solution [3]

$$c_f = \frac{0.664}{\sqrt{Re_x}}$$

The heat transfer solution for constant wall temperature was first obtained by Pohlhausen [18]. His solution can be approximated by correlation relations in three ranges. Only that in the intermediate Prandtl range is reported. This is

$$Nu_x = 0.332 \ Pr^{1/3} \ Re_x^{1/2} \qquad 0.5 < Pr < 10$$

The corresponding solution for uniform heat flux is given by

$$Nu_x = 0.453 \ Pr^{1/3} \ Re_x^{1/2} \qquad 0.5 < Pr < 10$$

In fluid flow at high velocities, the above relations remain valid if now the heat transfer coefficient h is defined as

$$h = \frac{q_w''}{T_w - T_{aw}}$$

where q_w'' = wall heat flux

The adiabatic wall temperature is given by

$$T_{aw} = T_\infty + r \frac{V_\infty^2}{2c_p} = T_\infty \left[1 + r \frac{\gamma - 1}{2} M^2 \right]$$

and the recovery factor r can be approximated by

$$r = Pr^{1/2} \qquad 0.5 < Pr < 5$$

3.3.1.2 Wedge Flow

The wedge flow skin friction and heat transfer coefficients are functions of the exponent m of the external velocity distribution. Eckert [7] gives

$$c_f = \frac{2}{\sqrt{2-\beta}} \frac{\Phi''(0)}{\sqrt{Re_x}}$$

where β is related to m by the equation

$$\beta = \frac{2m}{m+1}$$

and $\Phi''(0)$ can be approximated to less than 1% from the exact solution by

$$\Phi''(0) = 1.120(\beta + 0.2)^{0.53} \qquad (\beta > 0)$$

and

$$Nu_x = \frac{1}{\sqrt{2-\beta}} \Phi_t''(0) \sqrt{Re_x}$$

the values of $\Phi_t''(0)$ can be approximated to less than 2% from the exact solution by

$$\Phi_t''(0) = 0.56(\beta+0.2)^{0.11} \, Pr^{0.35+0.02\beta} \qquad (\beta \sim 0)$$

3.3.1.3 Cross-Flow Over Cylinders

It is necessary to distinguish between two cases depending on whether or not the body is symmetrical about an axis parallel to the stream at large distances from the body [22]. The velocity distributions for both cases have been obtained by Howarth using the Blasius series [3]. However, only the symmetric case has been treated when heat and mass transfer were incorporated.

The best approximation of the external velocity distribution is given by Eckert as [7]

$$\frac{u}{u_0} = 3.61 \left[\frac{x}{D}\right] - 3.275 \left[\frac{x}{D}\right]^3 - 0.1679 \left[\frac{x}{D}\right]^5 \qquad Re_D \sim 19000$$

where D = diameter of cylinder

Using this velocity distribution and the series tabulations of Froessling [12] Eckert obtained the following expression for the local Nusselt number, for air having a Prandtl number of 0.7

$$\frac{Nu}{\sqrt{Re_D}} = 0.9450 - 0.7696 \left[\frac{x}{D}\right]^2 - 0.3478 \left[\frac{x}{D}\right]^4$$

By using an expression for $\frac{u}{u_0}$ given by Hiemenz [13]

$$\frac{u}{u_0} = 3.6314 \left[\frac{x}{D}\right] - 2.1709 \left[\frac{x}{D}\right]^5 - 1.5144 \left[\frac{x}{D}\right]^5$$

Froessling obtained the following expression for $Nu/Re_D^{1/2}$

$$\frac{Nu}{\sqrt{Re_D}} = 0.9450 - 0.5100 \left[\frac{x}{D}\right]^2 - 0.5956 \left[\frac{x}{D}\right]^4$$

Froessling has also shown that for large Prandtl numbers, Nu is proportional to $(Pr)^{1/3}$ on the entire surface in the boundary layer. This same relation has been found experimentally to hold for values of Pr not very large. Thus, the above relation can be written more generally as

$$\frac{Nu}{\sqrt[3]{Pr}\ \sqrt{Re_D}} = 1.0042 - 0.5744 \left[\frac{x}{D}\right]^2 - 0.6708 \left[\frac{x}{D}\right]^4$$

Martinelli, et al. [17] studied the data of Schmidt and Wenner and proposed the following empirical equation for predicting the local Nusselt number on a cylinder up to $\theta = 80°$ in a flow having a main stream turbulence less than 1%

$$\frac{hD}{K} = 1.14\ (Pr)^{0.4}\ Re_D \left[1 - \left[\frac{\theta}{90}\right]^3\right]$$

Since the analytical solutions are unable to predict heat transfer in the separated region, the average Nusselt number is often more useful, especially when heat transfer from the whole cylinder is required. Douglas and Churchill [5] gave the following empirical correlation, which applies to gases only

$$Nu = 0.45 \ Re_D^{1/2} + 0.00128 \ Re_D$$

valid for $Re_D > 500$. Douglas and Churchill did not give any equation for $Re_D < 500$, but Hsu [15] has noticed that the equation suggested by Eckert and Soehngen correlates the data for $Re_D < 500$ accurately

$$Nu = 0.43 + 0.48 \ Re_D^{1/2}$$

For both the above correlations, the gas properties are to be evaluated at the film temperature, $0.5\left(T_w + T_\infty\right)$.

3.3.1.4 Sphere

For the pressure distribution obtained by Fage [11]

$$\frac{u}{u_0} = 3 \left[\frac{x}{D}\right] - 3.4966 \left[\frac{x}{D}\right]^3 + 4.7391 \left[\frac{x}{D}\right]^5 - 5.4181 \left[\frac{x}{D}\right]^7 .$$

Froessling obtained the following expression for the local Nusselt number

$$\frac{Nu}{\sqrt[3]{Pr}\sqrt{Re_D}} = 1.369 - 1.579 \ \frac{x}{D} + 1.81 \ \frac{x}{D}$$

Knudsen and Katz [16] recommended the following correlation for the prediction of average Nusselt numbers for flow of fluids past spheres

$$Nu_m = 2.0 + 0.60 \ Pr^{1/3} \ Re_D^{1/2}$$

This correlation is valid for wide ranges of Reynolds and Prandtl numbers:

$$0.6 < Pr < 400$$
$$1 < Re_D < 70,000$$

3.3.2 Turbulent Continuum Flow

For turbulent flow over a flat plate the skin friction is usually estimated from any of the empirical correlations. The most accurate of this is probably that due to Prandtl-Schlichting. This is of the form

$$\bar{c}_f = \frac{0.455}{(\log Re)^{2.58}}$$

The heat transfer coefficient is now obtained by any one of the many Reynolds analogies. These were listed extensively in Knudsen and Katz [16] and Schlichting [22]. The simplest of this is the Colburn analogy, given by

$$Nu = \frac{c_f}{2} Re \ Pr^{1/3}$$

Note that this applies also to laminar flow. Eckert [8] suggested that the fluid properties be evaluated at the temperature

$$T_e = \frac{0.1 \ Pr + 40}{Pr + 72} (T_w - T_\infty) + T_\infty$$

In laminar high velocity flow, we have come to the
conclusion that the same low velocity results remain
valid if we replace the low velocity driving potential
$T_w - T_\infty$ by $T_w - T_{aw}$. Since this conclusion is only
based on the linearity of the energy equation, the same
should also hold in turbulent flow. Thus the high
velocity problem again reduces to the determination of
the recovery factor. For Prandtl number in the neighbor
hood of unity (0.5 < Pr < 2), this is given by Ackermann
[1] as

$$r = Pr^{1/3}$$

For flow over a cylinder and a sphere, theoretical
solutions are available only in laminar flow. From
comparisons with experimental data, it is observed that
the free stream turbulence has a systematic influence
on the heat transfer coefficient. However, this varia-
tion has not been correlated.

3.3.3 Slip Flow

3.3.3.1 Flat Plate

Heat transfer to or from a flat plate in slip flow
has been investigated by Schaaf [36] as well as Drake
and Kane [29]. Both Schaaf and Drake and Kane obtained
solutions for a diatomic gas and an accommodation coeffi-
cient of 0.8. Their solutions are of the same form

59

Schaaf:

$$St = \frac{0.38}{Z_2^2 M} \left[\exp(Z_2^2) \, \text{erfc} \, Z_2 - 1 + \frac{2}{\sqrt{\pi}} Z_2 \right]$$

where St = average Stanton number = $\dfrac{\hbar}{\rho c_p u_\infty}$

and $Z_2 = \dfrac{\sqrt{Re \, Pr}}{2.63 \, M}$

Drake and Kane:

$$Nu = 0.52M \left\{ \exp(Z_3^2) \, \text{erfc} \, Z_3 - 1 + \frac{2}{\sqrt{\pi}} Z_3 \right\}$$

where Nu = average Nusselt number

and $Z_3 = \dfrac{\sqrt{Re \, Pr}}{1.162 M}$

Both results are obtained by neglecting the viscous dissipation. For gases having Prandtl number of 0.72, the continuum limits of these equations are

Schaaf: $Nu = 0.956 \sqrt{Re}$

Drake and Kane: $Nu = 0.429 \sqrt{Re}$

The Pohlhausen solution is

$$Nu = 0.594 \sqrt{Re}$$

Thus it is seen that both solutions yield wrong limiting values. Schaaf's solution is 1.612 times higher than the correct result whereas that of Drake and Kane is too low by a factor of 1.384. The actual solution may be expected to lie somewhere in between these two solutions.

3.3.3.2 Cylinder

Numerous experimental investigations had been con-
ducted in the slip flow regime using fine cylindrical
wires--mainly in connection with hot-wire anemometry.
A convenient summary of such experiments can be found
in reference [27], which also gave a series of over
1000 convective heat transfer coefficients for normal
cylinders in subsonic slip flow. Even with such an
extensive amount of data no correlation formulas have
been found. This is because now Nu = f(Re, M) or Nu =
f(Re, Kn). The same reference argued that the use of
Knudsen number as the second parameter in correlating
slip flow data is preferable. This preference identi-
fies the anaomalous behavior in slip flow as a "rare-
fied gas phenomenon" rather than as a "Mach number
effect" associated with compressibility. This prefer-
ence is supported by an analysis given by Sauer and
Drake [33] which is capable of predicting this
anomalous behavior using a simplified slip flow
analysis. However, the prediction of this approximate
analysis is not numerically exact, though qualitative
agreement is excellent. The local Nusselt number for
a constant wall temperature cylinder is given by

$$\frac{hD}{k} = DL \int_0^\infty \frac{e^{-xu^2}}{\left[\frac{\pi}{2}(DL)^{\frac{1}{2}}uJ_1(u) + \frac{\pi}{2}(DL)^{\frac{1}{2}}J_0(u)\right]^2 + \left[\frac{\pi}{2}(DL)^{\frac{1}{2}}uY_1(u) + \frac{\pi}{2}(DL)^{\frac{1}{2}}Y_0(u)\right]^2} \cdot \frac{du}{u}$$

where $\quad x = \dfrac{a\theta}{2VD}$

and $\quad \dfrac{1}{L} = 1.996 \left[\dfrac{\gamma}{\gamma+1}\right]\left[\dfrac{2-\alpha}{\alpha}\right] \dfrac{\lambda}{Pr}$

a = thermal diffusivity, ft^2/sec

θ = angle measured from forward stagnation point, rad.

$V = V_0/n \quad (n = 3)$

V_0 = free stream velocity, ft/sec

D = diameter of cylinder, ft

λ = mean free path, ft

u = dummy variable

J_n = Bessel function of order n of the first kind

Y_n = Bessel function of order n of the second kind

The average Nusselt number can be found by integrating over the surface of the cylinder. For small values of x_π (value of x for $\theta = \pi$), this can be approximated by the following expression:

$$Nu = DL\left[1 - \frac{4}{3\pi^2}(DL)x_\pi^{\frac{1}{2}} + \frac{DL}{4}(1 + 2DL)x_\pi + \ldots\right]$$

3.3.3.3 Sphere

Heat transfer to a sphere in slip flow has been reported by Drake and Kane [29]. The average Nusselt

number for a sphere having constant surface temperature
is given by

$$Nu = 2 + \frac{2}{\pi^2} \int_0^\infty \frac{(1 + e^{-\beta^2 \pi})(1 + \beta^4)^{-1} \, d\beta}{\left\{ [J_1(\alpha\beta) + N\alpha\beta J_2(\alpha\beta)]^2 + [Y_1(\alpha\beta) + N\alpha\beta Y_2(\alpha\beta)]^2 \right\} \beta}$$

where $\alpha = \sqrt{2Re \ Pr}$

and $N\alpha = \frac{8}{3} \left[1.996 \ \frac{2-\alpha}{\alpha} \ \frac{\gamma}{\gamma+1} \right] \frac{M}{\sqrt{2Re \ Pr}}$

β = dummy variable

The effects of compressibility and dissipation have been
neglected.

A simpler relation for practical application is
given by Kavanau and Drake [32]

$$Nu = \frac{Nu_0}{1.0 + 3.42 \left(\frac{M}{Re \ Pr} \right) Nu_0}$$

where the subscript "0" denotes values in continuum
flow.

3.3.4   Free Molecule Flow

In order to facilitate the comparison of the heat
transfer results with corresponding results in continuum
flow, free molecule flow results are most conveniently
expressed in terms of a modified thermal recovery factor
r' and a modified Stanton number St', first introduced
by Oppenheim [39], both of which depend only on the
speed ratio, S. These are defined as

$$r' = \frac{T_r - T_\infty}{T_0 - T_\infty} \frac{\gamma + 1}{\gamma}$$

and $\quad St' = \frac{Q}{A\rho U c_p (T_r - T_w)} \frac{\gamma}{\alpha(\gamma+1)}$

$$S = \frac{u}{\sqrt{2RT}} = \sqrt{\frac{\gamma}{2}}\, M$$

where $\quad Q$ = heat flow rate

$\quad T_0$ = stagnation temperature = $T_\infty \left(1 + \frac{\gamma - 1}{\gamma} S^2 \right)$

$\quad A$ = total heat transfer area

$\quad \alpha$ = accommodation coefficient

$\quad M$ = Mach number

and $\quad u$ = macroscopic gas velocity

Though the results quoted below have been traced to their original authors, these expressions have been put into the form suggested by Oppenheim, which reduces all relationships to a form common to all gases irrespective of their molecular structure. The same reference also described a method of applying these simple geometrical shapes to compound surfaces.

3.3.4.1 Flat Plate [43]

For a flat plate, at angle of attack 0, with front and rear surfaces in perfect thermal contact and with A equal to the total area on both sides of the plate, the values of r' and St' are

$$r' = \frac{1}{S^2}\left\{2S^2 + 1 - \frac{1}{1+\sqrt{\pi}(S \sin \theta)\mathrm{erf}(S \sin \theta)\exp[(S \sin \theta)^2]}\right\}$$

$$St' = \frac{1}{4\sqrt{\pi}S}\left\{\exp[-(S \sin \theta)^2] + \sqrt{\pi}(S \sin \theta)\mathrm{erf}(S \sin \theta)\right\}$$

For a flat plate, at angle of attack θ, with front and rear surfaces insulated from one another and A equal to the area of one side of the plate, we have for the front side

$$r' = \frac{1}{S^2}\left\{2S^2 + 1 - \frac{1}{1+\sqrt{\pi}(S \sin \theta)[1+\mathrm{erf}(S \sin \theta)\exp[S \sin \theta)^2]}\right\}$$

$$St' = \frac{1}{4\sqrt{\pi}S}\left\{\exp[-(S \sin \theta)^2] + \sqrt{\pi}(S \sin \theta)[1+\mathrm{erf}(S \sin \theta)]\right\}$$

For the rear side, we need only to replace θ by $(-\theta)$ in the above equations.

3.3.4.2 Right Circular Cylinder [44]

For the right circular cylinder with axis normal to the direction of flow and A the surface area without end contributions, r' and St' are given by

$$r' = \frac{(2S +3)I_0\left(\frac{S^2}{2}\right) + (2S^2+1)I_1\left(\frac{S^2}{2}\right)}{(S^2+1)I_0\left(\frac{S^2}{2}\right) + S^2 I_1\left(\frac{S^2}{2}\right)}$$

$$St' = \frac{\exp\left(+\frac{S^2}{2}\right)}{4\sqrt{\pi}}\left[\frac{S^2+1}{S} I_0\left(\frac{S^2}{2}\right) + SI_1\left(\frac{S^2}{2}\right)\right]$$

where I_0 and I_1 are the modified Bessel functions.

3.4.3 Sphere

For a sphere with A equal to the surface area,
Sauer [41] obtained the following relations

$$r' = \frac{(2S^2+1)\left[1 + \frac{1}{S} \text{ i erfc(S)}\right] + \frac{2S^2-1}{2S^2} \text{ erf(S)}}{S^2\left[1 + \frac{1}{S} \text{ i erfc(S)}\right] + \frac{1}{2S^2} \text{ erf(S)}}$$

$$St' = \frac{1}{8S^2}\left[S^2 + S \text{ ierfc(S)} + \frac{1}{2} \text{ erf(S)}\right]$$

where ierfc is the integrated complementary error function.

From these results, it may be observed that for all the three bodies, and for the frontal side of the insulated flat plate, the recovery factors are always greater than unity. Hence, in contrast to continuum flow the equilibrium temperature in free molecule flow is greater than the local stagnation temperature. This phenomenon has been verified experimentally by Stalder et al. [44] for a cylinder in both monatomic and diatomic gases.

3.4 Cited References

Continuum Flow

1. Ackermann, G., Forsch. Gebiete Ingenieurw., 13, 1942, p. 226

2. Ambrok, G. S., Sov. Phys.-Tech. Phys., 2, 1957, p. 1979.

3. Blasius, H., Z. Math. u. Phys., 56, 1908, p. 1. Engl. transl. in NACA TM 1256.

4. Deissler, R. G. and Loeffler, A. L., Jr., NACA TN 4262, 1958.

5. Douglas, W. J. M. and Churchill, S. W., Chem. Eng. Prog., Symp. Ser., 52: 18, 1956, p. 23.

6. Drake, R. M., JAS, 1953, p. 309.

7. Eckert, E. R. G., VDI Forschungsheft, 416, 1942, pp. 1-24.

8. Eckert, E. R. G., Introduction to the Transfer of Heat and Mass, McGraw Hill, 1950.

9. Eckert, E. R. G. and Drewitz, O., Forsch. Gebiete Ingenieurw., 11, 1940, p. 116.

10. Emmons, H. W. and Brainerd, J. G., J. Appl. Mechs., 8, A 105, 1941 and 9, A1, 1942.

11. Fage, A., ARC R & M 1766, 1937.

12. Froessling, N., NACA TM 1432, 1958.

13. Hiemenz, Diss. Göttingen, 1911; Dinglers Polytechn. J., 326, 1911, p. 321.

14. Howarth, L., Proc. Roy. Soc. London, A194, 1948, p. 16.

15. Hsu, S. T., Engineering Heat Transfer, Van Nostrand, 1963, p. 332.

16. Knudsen, J. G. and Katz, D. L., Fluid Dynamics and Heat Transfer, McGraw-Hill, 1958.

17. Martinelli, R. C., Ginbert, A. G., Morrin, E. H., and Boelter, L. M. K., NACA WR W-14, 1943.

18. Pohlhausen, E., ZAMM, 1, 1921, pp. 115-21.

19. Reshotko, E. and Tucker, M., NACA TN 4154, 1957.

20. Reynolds, W. C., Kays, W. M. and Kline, S. J., NASA Memo 12-3-58W, 1958.

21. Rubesin, M. W., NACA TN 2345, 1951.

22. Schlichting, H., Boundary Layer Theory, McGraw Hill, 6th ed., 1968.

23. Spalding, D. B., JFM, $\underline{4}$, Part 1, May 1958, p. 22.

24. Spalding, D. B., ASME/I. Mech. E. Joint Heat Transfer Conf., 1961, Boulder, Colo.

25. Spalding, D. B. and Pun, W. M., Int. J. Heat Mass Transfer, $\underline{5}$, 1962, p. 239.

26. Van Driest, E. R., NACA TN 2597, 1952.

Slip Flow

27. Baldwin, L. V., NACA TN 4369, 1958.

28. Burnett, D., Proc. London Math. Soc., $\underline{40}$, 1935, p. 382.

29. Drake, R. M. and Kane, E. D., ASME/I. Mech. E. Gen. Disc. on Heat Transfer, London, 1951, pp. 117-21.

30. Devienne, F. M., Adv. in Heat Transfer, $\underline{2}$, 1965, pp. 272-356.

31. Grad, H., Comm. on Pure and Appl. Math., $\underline{2}$, 1949, p. 331.

32. Kavanau, L. L., and Drake, R. M., Jr., Univ. Calif. Inst. Engrg. Res. Rept. HE-150-108, 1953. See also Kavanau, L. L., ASME Trans., $\underline{77}$, no. 5, 1955. Also discussed in detail in Eckert and Drake, pp. 285-9.

33. Sauer, F. M., and Drake, R. M., Jr., JAS, $\underline{20}$, 1953, pp. 175-80.

34. Schaaf, S. A. and Chambre, P. L., Section II of Fundamentals of Gas Dynamics, H. W. Emmons ed., Vol. III, Princeton Series on High Speed Aerodynamics and Jet Propulsion, 1958, pp. 689-90.

35. op. cit., p. 719.

36. Schaaf, S. A., Heat Transfer, A. Symposium, 1952, Engr. Res. Inst., Univ. of Michigan.

Free Molecule Flow

37. Jaffe, G., Ann. Physik, $\underline{6}$, 1930, p. 195.

38. Liu, C. Y. and Lees, L., in Rarefied Gas Dynamics, L. Talbot, ed. Acad. Press, 1961, pp. 391-428.

39. Oppenheim, A. K., JAS, 20, 1953, p. 49.

40. Probstein, R. F., In Theory and Fundamental Research in Heat Transfer, Proc. ASME Annual Meeting, New York, Nov. 1960, J. A. Clark, ed., p. 59.

41. Sauer, F. M., JAS, 18, 1951, p. 353.

42. Schaaf, S. A., in Developments in Heat Transfer, W. M. Rohsenow, ed., p. 138-9.

43. Stalder, J. R., and Jukoff, D., JAS, 15, 1948, pp. 381-91; also NACA Rept. 944, 1949.

44. Stalder, J. R., Goodwin, G. and Creager, M. O., NACA TN 2244, 1950, and NACA TN 2438, 1951.

45. Stickney, R. E., Phy. Fluids, 5, 1962, pp. 1617-24.

IV.   EFFECT OF DIFFERENT MARTIAN ATMOSPHERIC
MODELS ON THE CONVECTIVE HEAT TRANSFER COEFFICIENTS
OF A SURFACE LANDER

The determination of the convective heat transfer
coefficient for the Martian atmosphere requires the
consideration of the following factors.

1. An accurate atmospheric model. This is
    required in order that thermal and transport
    properties as well as the operating Mach and
    Reynolds numbers can be accurately predicted.

2. A criterion for evaluating which flow regime
    will occur under the given atmospheric condi-
    tions.

3. The behavior of the transport properties of
    a gas at low pressures.

The last factor has been considered previously in
the Survey of Thermal and Transport properties. The
decrease in the apparent viscosity has been attributed
to slip over/the confining surfaces and the bulk vis-
cosity of the gas away from the surface has been assumed
to remain constant at the nominal value predicted by the
Kinetic Theory. The validity of this statement is
heuristically assumed in the present investigation.

However, this can be checked experimentally by means of a velocity survey under slip flow conditions. If the measured profile agrees with that predicted based on the above assumption, then t'e uncertainty associated with this statement will be conclusively removed. Up to now, no such profiles have been reported, at least to the knowledge of the authors. This problem, being of a fundamental nature, surely deserves investigation.

Much discussion has been reported on Factor 2; how ever, no conclusion has been reached. This is because most of these discussions are also of a heuristic nature and not based on experimental observations. It will be shown that from the experimental results of reference [3], a criterion for this subdivision can be deduced. The evaluation of the flow regime will be based on this criterion deduced here.

Finally, the uncertainty about the atmospheric models can only be resolved by direct measurement. This is beyond the scope of the present investigation. Therefore, it is proposed to evaluate the heat transfer coefficients for all the proposed models to determine the extent of their effects. A tabulation of these proposed atmospheric models is given in Table 4.1

4.1 Estimation of Boundary Between Continuum and Slip Flow

The division of gas dynamics into various flow regimes, based on values of the ratio λ/h., where λ is

Table 4.1 Martian Atmospheric Models

Property	Symbol	Dimension	VM-1	VM-2	VM-3	VM-4	VM-5	VM-6	VM-7	VM-8	VM-9	VM-10
Surface Pressure	P_0	mb	7.0	7.0	10.0	10.0	14.0	14.0	5.0	5.0	20.0	20.0
		lb/ft²	14.6	14.6	20.9	20.0	29.2	29.2	10.4	10.4	41.7	41.7
Surface Density	ρ_0	(gm/cm³)10³	0.955	1.85	1.365	2.5	1.91	3.08	0.68	1.32	2.73	3.85
		(slugs ft³)10⁵	1.85	3.59	2.65	4.98	3.7	5.97	1.32	2.56	5.30	7.44
Surface Temperature	T_0	°K	275	200	275	200	275	200	275	200	275	200
		°R	495	360	495	360	495	360	495	360	495	360
Stratospheric Temperature	T_s	°K	200	100	200	100	200	100	200	100	200	100
		°R	360	180	360	180	360	180	360	180	360	180
Acceleration of Gravity at Surface	g	cm/sec²	375	375	375	375	375	375	375	375	375	375
		ft/sec²	12.3	12.3	12.3	12.3	12.3	12.3	12.3	12.3	12.3	12.3
Composition (percent)												
CO₂ (by mass)			25.2	100.0	28.2	70.0	25.2	35.7	28.2	100.0	26.2	15.2
CO₂ (by volume)			20.0	100.0	20.0	68.0	20.0	29.4	20.0	100.0	20.0	9.5
N₂ (by mass)			71.8	0.0	71.8	0.0	71.8	28.6	71.8	0.0	71.6	63.0
N₂ (by volume)			90.0	0.0	80.0	0.0	80.0	52.2	90.0	0.0	80.0	70.5
A (by mass)			0.0	0.0	0.0	30.0	0.0	35.7	0.0	0.0	0.0	25.0
A (by volume)			0.0	0.0	0.0	32.0	0.0	34.2	0.0	0.0	0.0	20.0
Molecular Weight	M	mol⁻¹	31.2	44.0	31.2	42.7	31.2	34.4	31.2	44.0	31.2	32.1
Specific Heat of Mixture	C_p	cal/gm°C	0.230	0.166	0.230	0.2350	0.235	0.2713	0.230	0.166	0.230	0.2207
Specific Heat Ratio	a		2.35	1.37	1.39	1.43	1.35	1.45	1.36	1.37	1.36	1.41
Adiabatic Lapse Rate	Γ	°K/km	-3.95	-5.39	-3.86	-5.85	-3.55	-3.42	-3.86	-5.39	-3.64	-4.35
		°R/1000 ft	-2.13	-2.96	-2.13	-3.21	-2.23	-2.85	-2.13	-2.96	-2.13	-2.35
Tropopause Altitude	h_T	km	19.3	19.6	19.3	17.1	19.3	19.4	19.3	18.6	19.3	23.2
		kilo ft	63.3	61.0	63.3	56.1	63.3	21.6	63.3	61.0	63.3	75.5
Inverse Scale Height (stratosphere)	s	km⁻¹	0.0705	0.199	0.0705	0.2393	0.0705	0.2833	0.0705	0.199	0.0705	0.145
		ft⁻¹×10³	2.15	6.07	2.15	5.89	2.23	5.03	2.15	6.07	2.15	4.41
Continuous Surface Wind Speed	$\bar{v}$	ft/sec	186.0	186.0	155.5	155.5	232.3	232.3	220.0	220.0	110.0	110.0
Maximum Surface Wind Speed	v_{max}	ft/sec	470.0	470.0	390.0	390.0	356.0	332.0	556.0	556.0	278.0	278.0
Design Vertical Wind Gradient	$\frac{dv}{dh}$	ft/sec/1000 ft	2	2	2	2	2	2	2	2	2	2
Design Gust Speed	v_g	ft/sec	200	200	150.0	130.0	130.0	130.0	200.0	200.0	100.0	100.0

the mean free path and L a characteristic dimension of the system, was first proposed by Tsien [3]. Thereafter many sets of values of this parameter, which has now been named the Knudsen number, for defining the boundaries of the flow regimes have been introduced. The various criteria which have been suggested are in some disagreement, as all of these are mainly based on heuristic assumptions.

Starting from the equation used for computing the slip coefficient of a gas from viscosity measurements in a symmetric oscillating disk viscosimeter, it can be shown that by making a well-defined assumption on the slip phenomenon, the boundary between continuum and slip flow regimes can be established. In addition, the same set of experimental viscosity data can also be used to deduce the upper boundary of free molecule flow. Though this still does not provide a precise delimitation-- because the apparent viscosity measured under slip may depend on the geometry of the viscosimeter, we are at least in a better position to evaluate when slip should be taken into account in gas dynamics and heat transfer problems. If this criterion turns out to provide a good estimate, then it will be obviously natural for us to refer all apparent viscosity measurements from other viscosimeters to the form considered here.

The equations for computing the slip coefficient ζ from measurements in a symmetric oscillating disk viscosimeter is given in reference [3] as

$$\zeta = \frac{d}{2}\left[\left(\frac{\eta}{\eta_p}\right) - 1\right] \tag{1}$$

where η = nominal viscosity of gas, predicted by the kinetic theory

η_p = apparent viscosity of gas, value measured in symmetric oscillating disk viscosimeter under rarefied conditions

and d = spacing between rotating and fixed disks.

Maxwell [5] has shown that the slip coefficient almost equals the mean free path λ, for slip over smooth surfaces. Hence, we may write

$$\lambda = \frac{d}{2}\left[\left(\frac{\eta}{\eta_p}\right) - 1\right]$$

But, d is also the characteristic dimension L of the apparatus. We, therefore, obtain the following expression for λ/L

$$\frac{\lambda}{L} = \frac{1}{2}\left[\left(\frac{\eta}{\eta_p}\right) - 1\right] \tag{2}$$

Now, if we arbitrarily define the incipience of slip to be the point where the apparent viscosity falls outside the precision limits of reliable correlation formulas or theoretical predictions--these limits usually

vary, depending on the nature of the gas; for common gases, this may be taken to be 2 per cent--then, continuum flow occurs when

$$\frac{\lambda}{L} < \frac{1}{2}[1.02 - 1]$$ (3)

It should be pointed out that this definition of slip is by no means precise. A 2 percent deviation from the nominal value may be too severe a condition for gases having polar and complex molecules. For deviations of the apparent viscosity close to 2 percent, or for λ/L close to .01, the continuum theory may still be used as a good approximation. On the other hand, we should realize that slip occurs only under slight rarefaction, the upper limit of the slip flow regime cannot be easily estimated, and we, therefore, have no means of knowing at what value of the deviation shall we cease to apply the continuum approximation.

It is seen that the order of this magnitude corresponds to the criteria proposed by Schaaf and Chambre [6]. However, to be of any practical value, we should write the M/Re and $M/\sqrt{Re}$ ratios in a more precise form than merely use an order of magnitude analysis.

Recall that

$$\frac{\lambda}{L} = \left(\frac{\pi\gamma}{2}\right)^{\frac{1}{2}} \frac{M}{Re_L}$$

For a diatomic gas, this becomes

$$\frac{\lambda}{L} = 1.484 \ \frac{M}{Re_L} \tag{4}$$

Hence,

$$\frac{M}{Re_L} < .00674 \tag{5}$$

If the Reynolds number is large enough that boundary layer analysis is valid, then the characteristic length of the system is δ. But

$$\frac{\delta}{\ell} = \frac{5.0}{\sqrt{Re}_\ell}$$

where ℓ = length of plate corresponding to a boundary
layer thickness of δ.

Hence,

$$\frac{M}{\sqrt{Re}_\ell} < .0337 \tag{6}$$

From the same experimental data, the incipience of free molecular flow can also be deduced, as follows. The free molecule viscosity Z of a gas between two parallel plates is given by Kennard [4] as

$$Z = \frac{P}{(2\pi RT)^{\frac{1}{2}}} \tag{7}$$

where the parameters are defined by standard notations. Figure 8 of reference [3] shows that the apparent viscosity obeys the above relation closely for Z smaller than 400×10^{-7} poise. As the nominal viscosity, as

predicted by kinetic theory, is a function of temperature,
it is therefore seen from equation (2) that the Knudsen
number at which free molecular flow occurs depends on
the temperature of the system. It should be noted that
the incipient free molecule viscosity may differ for
different gases, because there exists at present insuffici-
ent evidence to generalize the above observation that the
value of η_p (= 400 × 10^{-7} poise) below which equation (7)
is valid applies to all other gases as well. As the gases
used in reference [3] were nitrogen and air which have
molecular weights differing but little from each other,
the difference in η_p, if any, is so very small as to be
indiscernable from their data. Until sufficient data
has been accumulated to provide a definite answer to this
question, it may be assumed to remain constant at
400 × 10^{-7} poise. Just to get an order of magnitude for
this value, let us take $\eta_{nominal}$ to be 1600 × 10^{-7} poise.
Equation (2) immediately gives

$$\frac{\lambda}{L} > 1.5$$

Thus, equation (4) gives

$$\frac{M}{Re_L} \sim 1.0$$

This criterion compares favorably with those suggested
by Stalder, Goodwin and Creager [7] and Schaaf and
Chambre [6]. It should be realized that this varies

with the temperature and probably also with the structure of the gas--both $\frac{\lambda}{L}$ and $\frac{M}{Re_L}$ decrease as temperature decreases.

In recapitulation, we have the following classification criterion:

Continuum Flow

$$\frac{\lambda}{L} < .01$$

Free Molecule Flow

$$\frac{\lambda}{L} \gtrsim 1.5$$

Alternatively, this can be expressed in terms of ratios involving the Mach and Reynolds numbers. However, now the ratios depend on the atomicity of the gases. For diatomic gases, this criterion becomes

Continuum Flow

$$\frac{M}{Re_L} < .00674 \; , \quad Re_L \sim O(1)$$

$$\frac{M}{\sqrt{Re_\ell}} < .0337 \; , \quad Re_\ell \gg 1$$

Free Molecule Flow

$$\frac{M}{Re_L} \gtrsim 1.0$$

It should be pointed out that the free molecule limit is a function of temperature. This classification

lowers the free molecule limit to the point that it almost eliminates the ill-defined regime usually designated as the transition regime. The validity of the above classification remains to be verified by more experimental evidence. The data given in Figure 5 of reference [7] already seem to indicate the validity of the free molecule limit.

From the atmospheric properties tabulated in Table 4.1, we see that the maximum Mach number than can occur is 0.745. Since the value of γ of the gas mixtures are all close to 1.4, the Reynolds number range in which continuum flow occurs is approximately given by

$$Re_\ell > \left[\frac{74.5}{3.37}\right]^2 = 490$$

Also, from the same table, the Reynolds number based on a length of 5 ft is of the order of 10^5. It is, therefore, seen that slip flow is of no importance in the analysis, and the continuum flow analysis should be valid except at the immediate vicinity of the leading edge. Also, from the Reynolds number tabulation, the flow is seen to be laminar, unless there exists an adverse pressure gradient.

4.2 Effects of Martian Atmospheric Models on Heat Transfer Coefficients

Having established the flow regime under the given atmospheric conditions, the heat transfer coefficients h

can be calculated from the corresponding solutions. As exact solutions for both laminar flow over a flat plate and a cylinder exist, it is, therefore, more expedient to calculate h from these existing results.

The mean heat transfer coefficient over a flat plate is given by

$$\overline{h} = .664 \ k \ PR^{\frac{1}{3}} \left(\frac{\rho u_\infty}{\mu}\right)^{\frac{1}{2}} \frac{1}{L^{\frac{1}{2}}} \tag{7}$$

Denoting the value of h for a plate of length L ft by h(L), and that for a length of 1 ft by h(1), we have

$$\overline{h}(L) = \frac{\overline{h}(1)}{\sqrt{L}} \tag{8}$$

where $\overline{h}(1) = .664 \ k \ Pr^{\frac{1}{3}} \left(\frac{\rho u_\infty}{\mu}\right)^{\frac{1}{2}}$

Assuming the Prandtl number for the different models to be constant at 0.72, the flat plate relation gives

$$\overline{h}(1) = 0.595 \ k \left(\frac{\rho u_\infty}{\mu}\right)^{\frac{1}{2}} \tag{9}$$

For the cylinder, the exact solution of the local heat transfer coefficient given by Eckert [1] for air is

$$\frac{Nu}{\sqrt{Re}} = 0.9450 - 0.7696 \left(\frac{x}{D}\right)^2 - 0.3478 \left(\frac{x}{D}\right)^4 \tag{10}$$

where Nu and Re are parameters based on D, the diameter of the cylinder and x is the distance measured along the circumference. As the Prandtl number for air is not very different from that of the gases in the different models,

the error incurred by using this expression is not very large.

Substituting for Nu and Re, we have

$$h_0 = k\left(\frac{\rho u_\infty}{\mu}\right)^{\frac{1}{2}} \frac{1}{D^{\frac{1}{2}}} f(\theta)$$

where $f(\theta) = 0.9450 - 0.7696 \left(\frac{x}{D}\right)^2 - 0.3478 \left(\frac{x}{D}\right)^4$

and $\quad\quad \theta$ = angle measured from forward stagnation point

$$= \frac{2x}{D}$$

Similarly, by defining a unit coefficient for $D = 1$ ft, we have

$$h_0(D) = \frac{h(1)}{\sqrt{D}} \tag{11}$$

where

$$h_0(1) = k\left(\frac{\rho u_\infty}{\mu}\right)^{\frac{1}{2}} f(\theta) \tag{12}$$

Equations (9) and (12) are seen to be similar, the effect of the different models will, therefore, be identical in both cases. The values for $\bar{h}(1)$ and $h_\theta(1)$ have been tabulated in Table 4.2. These calculations were based on the continuous wind speed and a free stream having properties of the Martian surface.

Since the analytical solutions are unable to predict heat transfer in the separated region, the average heat transfer coefficient cannot be obtained by integrating the values of h_0 over the cylinder. In order to calculate the average coefficients, empirical relations must be

used. No single equation has been found for correlating
all data over the entire Reynolds number range from 2 to
250,000. The best representation is given by the follow-
ing two equations reported by Hsu [2]

$$\overline{Nu} = 0.46 \, Re_D^{1/2} + 0.00128 \, Re_D \qquad Re_D > 500$$

and

$$\overline{Nu} = 0.43 + 0.48 \, Re_D^{1/2} \qquad Re_D \cdot 500$$

In using these relations, the gas properties are to be
evaluated at the film temperature. Values of the average
heat transfer coefficients from a cylinder one foot in
diameter for the different atmospheric models have also
been tabulated in Table 4.2. The comparison of the pre-
dictions or correlations with experimental data obtained
in a low density wind tunnel at the Jet Propulsion Labora-
tory in Pasadena, California is discussed in Chapter VI.

4.3 Concluding Remarks

The following conclusions can be drawn from the
preceding discussions.

1. A criterion for classifying the flow regimes
   has been arrived at based on the apparent
   viscosities measured by a symmetric oscillat-
   ing disk viscosimeter at low pressures.

2. Based on this criterion, the flow and heat
   convection in a Martian atmosphere over an

82

Table 4.2 Heat Transfer Coefficients for Various Martian Atmospheric Models

	Dimension	Atmospheric Model Number
		1	2	3	4	5	6	.	8	9	10
Surface Density	gm/cm³ 10⁵	0.955	1.85	1.365	2.57	1.91	3.06	0.65	2.35	2.7	3.83
Surface Temperature	K	275	200	275	205	275	200	275	200	275	200
	K	495	360	495	360	495	360	495	360	495	360
c_p	cal/gm°C	0.232	0.166	0.230	0.153	0.230	0.174	0.230	0.166	0.230	0.220
μ	(gm/cm sec)10⁸	15.926	10.177	15.926	11.667	15.926	13.02	15.926	10.177	15.926	13.177
k	(cal/cm sec°K)10⁶	50.819	23.435	50.819	35.072	50.819	35.408	50.819	23.435	50.819	58.19
Pr at surface		0.721	0.735	0.721	0.711	0.721	0.721	0.721	0.735	0.721	0.714
Continuous Wind Speed	ft/sec	156.0	186.0	155.5	155.5	151.5	151.5	220.0	220.0	210.0	110.0
Maximum Wind Speed	ft/sec	470.0	470.0	390.0	390.0	330.0	330.0	556.0	556.0	275.0	278.0
Re (based on continuous wind speed and L = 5 ft)	10⁻⁷	.526	1.573	.626	1.59	.742	1.45	.442	1.35	.585	1.485
Mach number (based on continuous wind speed)		.178	.249	.149	.201	.126	.156	.211	.295	.105	.124
Mach number (based on maximum wind speed)		.451	.630	.374	.504	.316	.392	.333	.743	.64	.313
Heat Transfer Coefficient											
Flat Plate: $\bar{h}$	Btu/hr ft² °R	0.737	0.605	0.803	0.644	0.676	0.786	0.603	0.552	0.955	0.945
Cylinder: $\theta = 0$	Btu/hr ft² °R	1.17	.955	1.174	1.022	1.392	1.21	1.17	.676	1.520	1.50
$\theta = 20$	Btu/hr ft² °R	1.14	.942	1.233	0.997	1.357	1.188	1.243	.855	1.492	1.452
$\theta = 40$	Btu/hr ft² °R	1.35	.865	1.142	.936	1.24	1.091	.959	.785	1.365	1.345
$\theta = 60$	Btu/hr ft² °R	.85	.724	.955	.766	1.041	.913	.601	.657	1.139	1.124
$\theta = 90$	Btu/hr ft² °R	.603	.498	.658	.527	0.718	.658	.552	.452	.785	.75
S.P.	Btu/hr ft² °R	.599	.693	.654	.744	0.713	.875	.550	.619	1.015	1.083

immersed body is found to be in the laminar
continuum regime.

3. The heat transfer coefficients for the differ-
ent atmospheric models do not vary very sig-
nificantly. For a flat plate, it lies between
a low value of 0.552 Btu/ft^2 hr°F for Model 8
and a high value of 0.958 Btu/ft^2 hr°F for
Model 9. For a cylinder in cross flow, the
local unit values are in the same ratio as
for the flat plate, and of the same order of
magnitude. However, the effect of the differ-
ent atmospheric models on the average heat
transfer coefficients for the cylinder are not
similar to that on the flat plate and the local
values on the cylinder before separation. This
is b cause these average values depend also on
the structure of the wake as well as the posi-
tion of separation.

4.4 Cited References

1. Eckert, E. R. G., Die Berechnung des Wärmeübergangs
    in der laminaren Grenzschicht umströmter Körper,
    VDI Forschungsheft 416, Bd. 13, 1942, p. 15.

2. Hsu, S. T., Engineering Heat Transfer, Van Nostrand,
    1963, pp. 330-2.

3. Johnston, H. L., Mattox, R. W. and Powers, R. W.,
    Viscosities of Air and Nitrogen at Low Pressures,
    NACA TN 2546, 1951.

4. Kennard, E. H., Kinetic Theory of Gases, McGraw-
    Hill, 1938, p. 300.

5. Maxwell, J. C., Illustrations on the Dynamical
   Theory of Gases--Part I. On the Motions and Col-
   lisions of Perfectly Elastic Spheres. Phil. Mag.,
   19, 1860 pp. 18-32, see also Collected Works,
   Vol. 2, Cambr. UP (London), 1890.

6. Schaaf, S. A. and Chambre, P. C., Flow of Rarefied
   Gases, In Section II of Fundamentals of Gas Dynamics,
   Vol. 3 of Princeton Series on High Speed Aerodynamics
   and Jet Propulsion, 1958, pp. 689-90.

7. Stalder, J. R., Goodwin, G. and Creager, M. O.,
   Heat Transfer to Bodies in a High Speed Rarefied
   Gas Stream, Proc. of the General Discussion on
   Heat Transfer, London, Sept. 1951, pp. 143-9.

8. Tsien, H. S., Superaerodynamics, Mechanics of
   Rarefied Gases, JAS, 13, 1946, pp. 653-64.

V.   EXPERIMENTAL FACILITY AND TEST PROCEDURE

5.1   Experimental Facility

In separate runs, a flat plate and a cylinder were
mounted in an open-circuit, suction-type wind tunnel
installed inside a 16-foot long and 4-foot diameter low-
pressure chamber, Figures 5.1 and 5.2.   The 12×12×12 in.
test section of the tunnel was constructed of aluminum
with removable lucite sections for test model insertion
and support.

Details of the models are given in Figures 5.3 and
5.4.   For the flat plate, the heat transfer surface was
composed of 9 Kapton Thermofoil heaters (Minco Products
Co., Minneapolis), coated with pressure-sensitive adhes-
ive and mounted in three rows of three heaters to one
side of a 1/4" thick 6061 T6 Aluminum plate, having a
highly polished surface finish on the other side.   The
entire model was constructed and assembled by Research
Service Co., Minneapolis in the following manner: A
thick layer of Fiberglass Strand insulation was "sand-
wiched" between two of the above-mentioned plates.   They
were fastened together with 14 counter-sunk flat heat
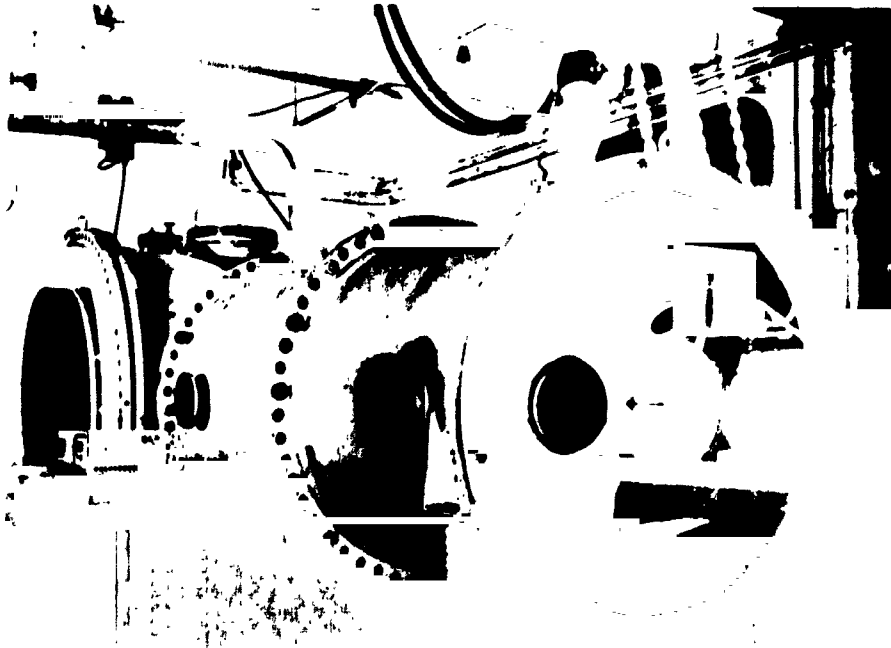screws onto a u-shaped canvas - laminated phenolic bonding
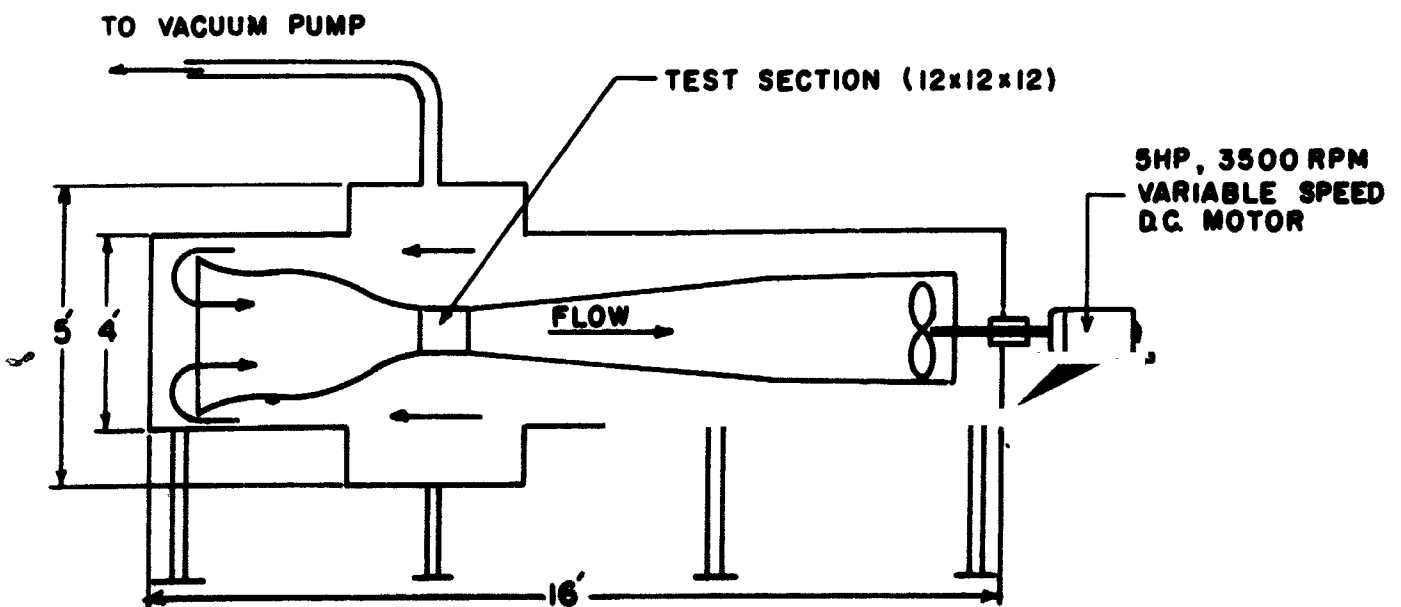
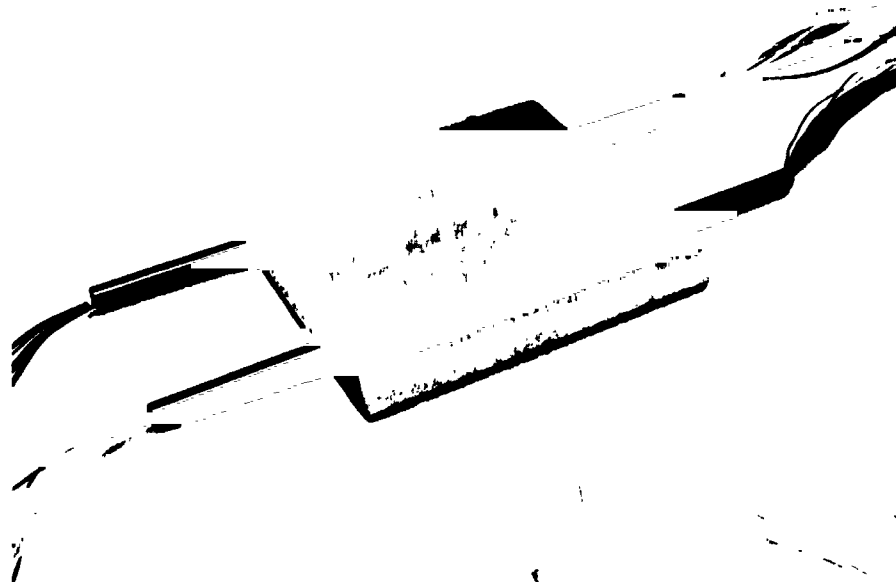Figure 5.1   JPL Low-Density Wind Tunnel Chamber

TO VACUUM PUMP

TEST SECTION (12×12×12)

5HP, 3500 RPM
VARIABLE SPEED
D.C. MOTOR

FLOW

5 4

16'

Figure 5.2   Schematic Diagram of Low-Density Wind Tunnel
at Jet Propulsion Laboratory, Pasadena

5.3a   Photograph of Flat Plate

- SUPPORTS
- 16 THERMOCOUPLES (V)
- 2" x 2" KAPTON GUARD HEATERS
- 3" x 2" KAPTON MAIN HEATERS
- 2" x 2" KAPTON GUARD HEATERS

8.10"

HEATERS   THERMOCOUPLES
- FIBERGLASS INSULATION
- 1/4" ALUMINUM
- PHENOLIC BONDING MATERIAL
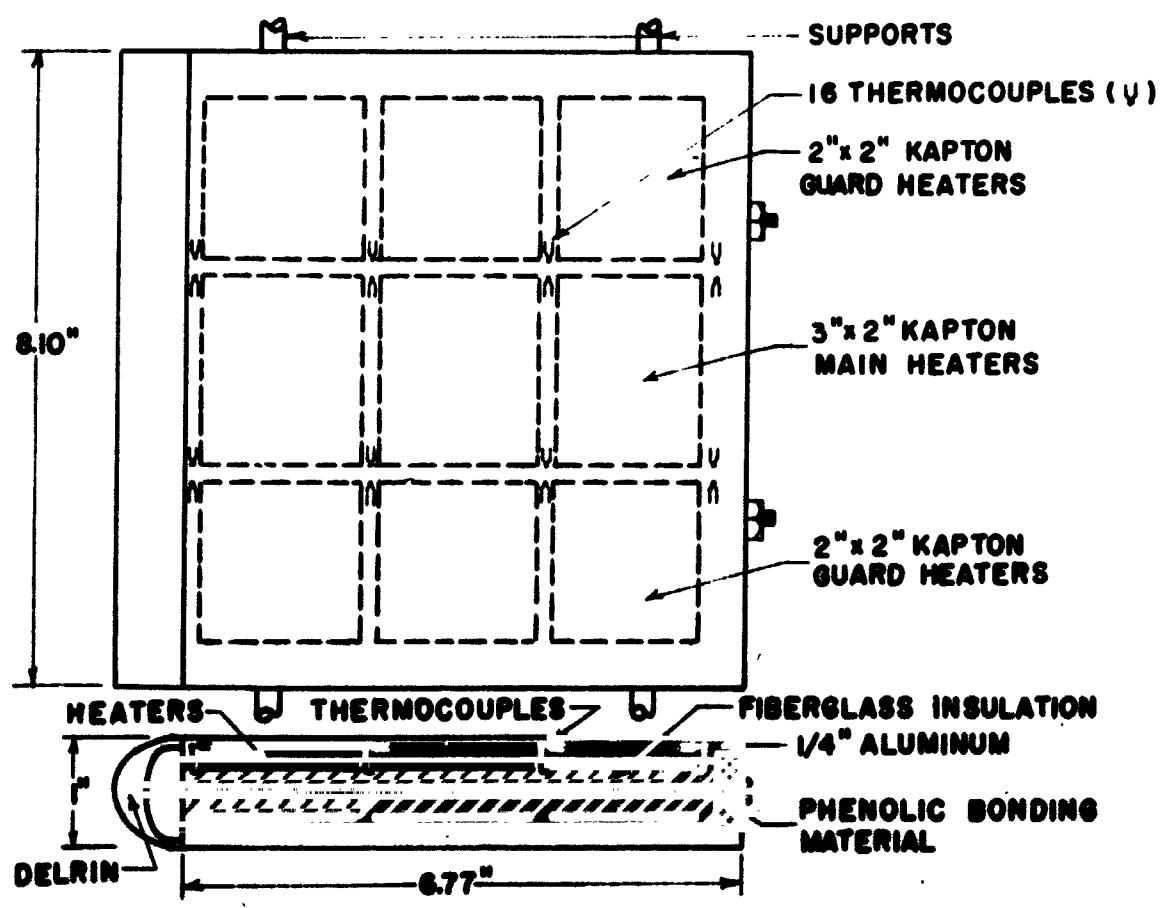
DELRIN
6.77"

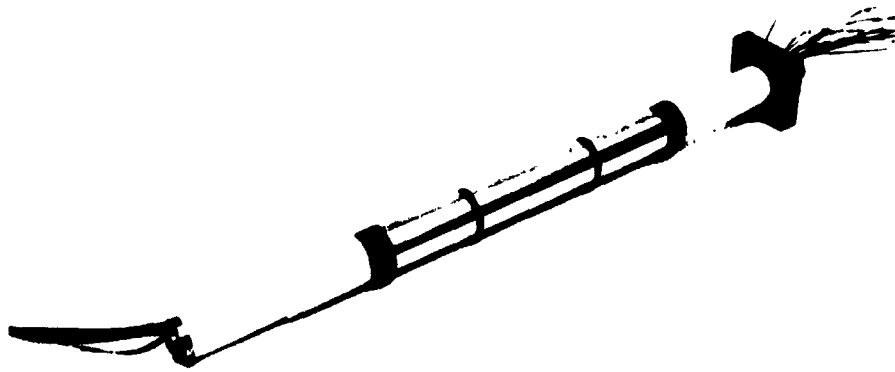Figure 5.3b   Schematic Cross-Section Diagram of Flat Plate

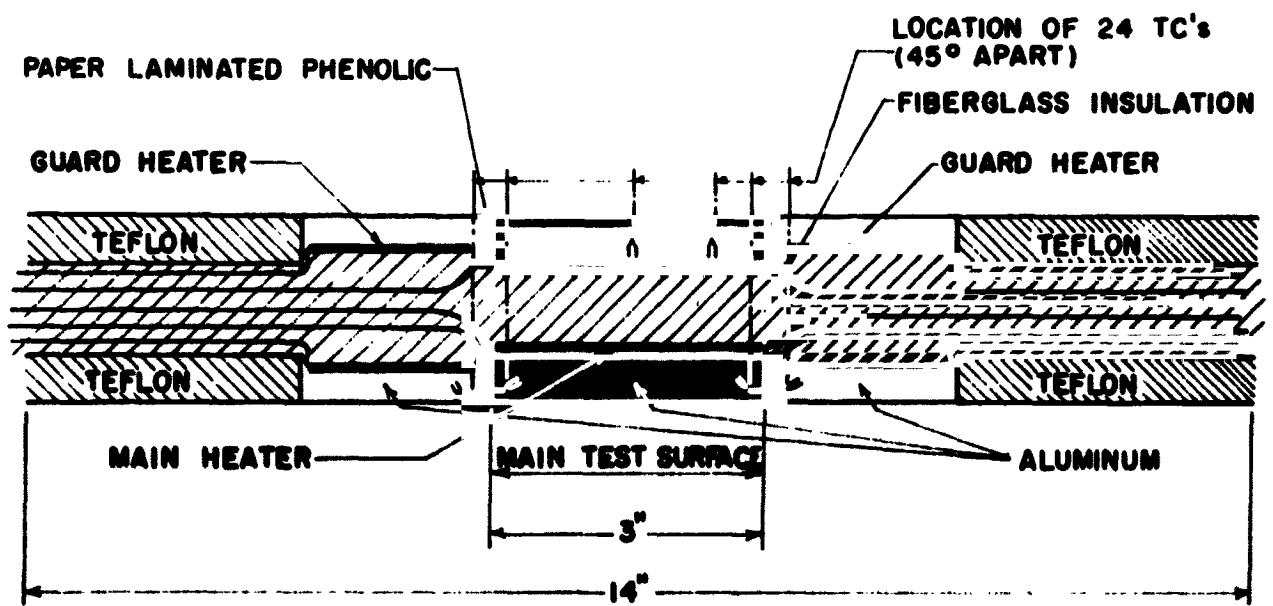Figure 5.4a   Photograph of Cylinder Specimen

Figure 5.4b   Schematic Diagram of Cylinder Cross-Section

material which enclosed the fiberglass insulation. The
hollow cylindrical nosepiece, made of Delrin, was drawn
flush against the upstream edge of the plates by two
rods. These rods were connected to the backside of the
nosepiece, ran through the center of the "sandwish," and
were tightened on the downstream part of the model.

The top plate, used for testing purposes, contained
16 thermocouples for surface temperature measurement.
They were bonded with copper oxide cement into small
holes drilled from the inside of the plate to within
1/16" of the polished test surface at strategic (for
calculating conduction losses) locations (see Figure
5.3b). All thermocouple and power leads were brought
out of the model through the four support rods attached
to the sides of the model.

Guard heaters were also used in constructing the
cylinder test specimen. The central section, employed
as testing surface, consisted of a 1" O.D., 1/2" I.D.
aluminum tube with a 3×2" cylindrical Kapton heater
pressed to the inside. A 1/8" long ring of paper-
laminated phenolic backing material and a guard heater
section, similar to the main section, were positioned
on each side to reduce the axial heat loss. Teflon
tubing on both sides protected the model from further
heat losses. All pieces were held together by a rod-
screw arrangement passing through the hollow, interior

of the test cylinder. The hollow interior was filled
with fiberglass insulation and served also to bring out
thermocouple and power leads. Surface temperatures
were measured with 24 30-gage chromel-constantan thermo-
couples placed at six cross-sectional locations (45°
apart) as close to the surface as possible (see Figure
5.4b). In order to avoid disturbances on the surface,
the thermocouples were inserted axially through slots
of circular cross section. The thermocouples fitted
snuggly into the axial slots and were bonded to the metal
with copper oxide cement.

Since the thermal resistance of the aluminum test
models is negligible in comparison to the convective
resistance of the external flow, the temperature measured
with the thermocouples below the surface can be assumed
to be equivalent to the surface temperature.

A three-dimensional traversing mechanism also con-
structed by Research Services, Minneapolis was used to
position the free-stream temperature and velocity probes
(see Figure 5.5). The cavity at the top of the wind
tunnel test section necessary for the travel of the probe
was closed by a thin sliding stainless steel plate mounted
flush with the top wall by means of small magnets. A
flexible shaft was attached to the positioner of the
traversing mechanism for remote control of the longitudi-
nal motion of the probe.

Figure 5.5   Wind Tunnel Test Facility

Free-stream temperature was measured with a chromel-constantan thermocouple aligned parallel to the stream and inserted into a 1/8" dia. tube (open end upstream) which was designed according to details given in Reference 1. This design minimized heat losses due to conduction, radiation and velocity.

A static and a total pressure probe of the Prandtl design was used to determine the free-stream velocity by reading the differential pressure in microbars, using a MKS Baratron Pressure Meter.

5.2 Test Procedures

The free-stream temperature and velocity of the gas were always taken well outside the boundary layers of the models. For the flat plate, the probes were positioned 1.5" above the geometrical center of the plate surface; for the cylinder they were located in the central plane bisecting the test section, 2" upstream and 1" above the top of the cylinder.

Velocity profiles taken in the horizontal and vertical direction indicated that for the entire length of the plate as well as for a sizeable distance upstream of the cylinder, the free-stream velocity varied less than 1% in that part of the stream unaffected by the test section walls.

From the latest Mariner probes which passed by Mars in August 1969, it was established that the Martian atmosphere is almost exclusively composed of CO_2. The pressure range due to uncertainties on the Martian surface was narrowed down to lie between 3.5 and 8.5 mm Hg. Consequently, the experimental plans were revised to take these developments into account, i.e., 100% CO_2 was used in all test runs and the pressures inside the chamber were kept within the range mentioned above.

For the experiments, the following procedure was employed: The chamber was evacuated, backfilled with

CO_2 gas numerous times to reach the desired purity, and
left overnight so that the pressure inside the chamber
would stabilize to the value of the desired total pres-
sure. In addition, the Baratron, used for measuring of
the velocity, also needed approximately 5-10 hrs. to
stabilize. Once the desired stabilization had been
accomplished, the motor driving the fan as well as the
power supply for the model was turned on simultaneously.
The fan speed was adjusted until the reading on the
Baratron indicated the calculated value for the desired
free-stream velocity and the power supplies were adjusted
to reach the anticipated steady-state surface temperature
(for a constant heat input) as fast as possible. The
reason for initially forcing the surface temperatures
to a higher value lay in the fact that the vacuum seal
bearings used in driving the fan were limited to 3 hrs.
of operation because of the danger of overheating.
Steady-state temperatures were usually reached in about
2 1/2 hrs. by frequently manipulating the power input,
thus "zeroing" in on the desired steady-state surface
temperatures.

At this point it should be noted that the power
input could be individually controlled to both guard
heating sections as well as the main heating section.
This was a relatively easy operation with the cylinder.
One power supply was used for heating the main test

surface while the other two supplied heat to the guard
sections which were constantly adjusted to keep the heat
loss $\left(\sim(T_{main}-T_{guard})\right)$ from the main section to a mini-
mum.

The flat plate heating procedure was more difficult.
Six power supplies instead of three were used, three
for heating of the top surface and three for the bottom
surface. The input to each of the latter three was
always kept equal to that of its corresponding heater
for the top surface, thus making the heat loss from the
top plate to the bottom plate negligible. It can be
seen from Figure 5.3b that both the top and bottom plates
have 9 heaters aligned in 3 "rows," each row consisting
of 3 heaters in the flow direction connected in parallel
to a power supply. The center row of heaters installed
in the top plate served for the heating of the main
"test" surface whereas all other heaters were used as
guard heaters in order to control the heat losses from
the main "test" surface. Thus, the greater fraction of
the main heater power input was carried away by convec-
tion from the "test" surface. Therefore, the guard
heaters were constantly adjusted to minimize the tem-
perature differences (and thus the heat loss) between
the "test" surface and the other parts of the model.

Power was provided by means of a multiple Datex
power supply which was connected to a 9500A RMS Digital

Voltmeter with which voltage and amperage could be read alternatingly for each heater. The Datex digital voltmeter, used for the print-out of the data from strategically-placed thermocouples, could be conveniently checked every 15 seconds (if so desired) so that appropriate adjustements in power input to the models could be achieved instantly to keep the surface temperatures at the desired values. Once the anticipated steady-state "test" surface temperature was approached, the test surface power supply was lowered to the input corresponding to that particular steady-state temperature; the guard heaters were also adjusted accordingly. "True" steady-state surface temperature was thought to be established when the difference between plate surface temperature and free-stream temperature was approximately constant over a period of 5 minutes. Maximum steady-state heat input was in all cases limited by the maximum temperature of 500°F allowed for the Kapton heaters.

The portion of the main heater input less the estimated losses is assumed to be carried away by the gas flowing over the heating surface. The heat losses are considered to be due to the following factors:

For the flat plate-

    a) Radiation from the heating surface of the specimen to the surroundings.

b) Conduction through the hollow nosepiece.

c) Conduction and convection to the wake of the plate.

d) Conduction from the main test surface to guard sections.

For the cylinder-

a) Radiation from the heating surface of the specimen to the surroundings.

d) Conduction from the main test surface to guard sections.

Loss (a) was calculated by Kirchhoff's and Stefan-Boltzmann's laws. Losses (b) and (c) were estimated by assuming a linear surface temperature profile in the flow direction at each end of the flat plate and assuming that its gradient is proportional to the corresponding heat loss. The heat loss (d) was also approximated by taking a linear temperature distribution between corresponding thermocouple readings at various locations between test and guard sections.

The four losses (a), (b), (c), and (d) added up to 40% of the total "test" surface heat input for the flat plate case but accounted for only 5% of the cylinder heat input. They were calculated individually for each test run with proper corrections.

The relatively high heat loss for the flat plate can be attributed to the fact that at low pressures and

therefore low forced convection heat transfer coefficients, the maximum heat input, limited by the maximum heater temperature, is quite low compared to the possible input at atmospheric pressures. Consequently, the relative heat loss at low pressures is quite pronounced. Radiation losses in either model accounted for approximately 3% of the main heat input; the greatest losses in the case of the flat plate were those of conduction through the nosepiece and convection to the wake of the plate.

Denoting the area of the "test" surface by A, the rate of main heat input by q_i, the sum of the heat losses by q_ℓ, the average surface temperature of the test surface by T_s, and the temperature of the free stream by T_∞, the average heat transfer coefficient by convection is found from the equation

$$\bar{h} = \frac{q_i - q_\ell}{A\left(T_s - T_\infty\right)}_{\text{steady-state}}$$

5.3 Cited Reference

1. Vickers, P. T., Proper Probes Keep Thermocouples Reading True, SAE Jour., Dec. 1964, pp. 54-57.

Table 6.1

Experimental Results

Page 98 Missing in Original Document

CYLINDER

p(mm Hg)	u_∞(fps)	q_ℓ (% q_i)	$\bar{h}_{exp}$ (Btu/hr ft²°F)	$\bar{h}_{comp}$ (Btu/hr ft²°F)	% differ-ence
4.55	88	5	1.48	1.37	+ 8
4.55	88	5	1.47	1.36	+ 8
4.55	129	3	1.78	1.60	+11
4.55	177	3	2.06	1.88	+10
4.55	212	3	2.21	2.08	+ 6
3.00	100	7	1.31	1.20	+ 9
6.00	88	4	1.69	1.51	+12
9.80	88	4	2.10	1.95	+ 8

FLAT PLATE

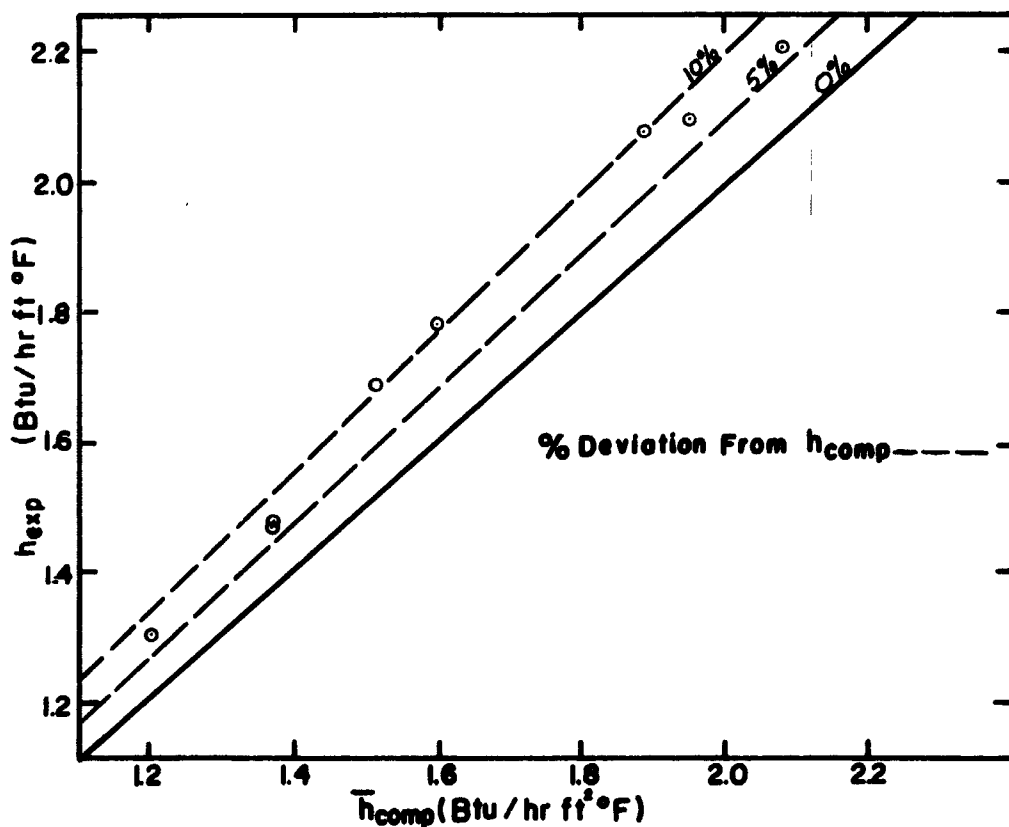| p(mm Hg)	u_∞(fps)	q_ℓ (% q_i)	$\bar{h}(1)_{exp}$ (Btu/hr ft²°F)	$\bar{h}(1)_{comp}$ (Btu/hr ft²°F)	% differ-ence
4.55	100	44	.48	.48	0
4.55	100	34	.53	.48	+10
4.55	150	32	.69	.59	+17
4.55	150	40	.55	.59	- 7
4.55	200	41	.71	.68	+ 4
4.55	200	40	.64	.68	- 6
4.55	230	38	.72	.73	- 1
4.55	230	36	.71	.73	- 3
3.10	150	41	.54	.49	+10
6.20	150	36	.66	.69	- 2

Figure 6.1   Graph of $\bar{h}_{exp}$ vs. $\bar{h}_{comp}$ for Cylinder
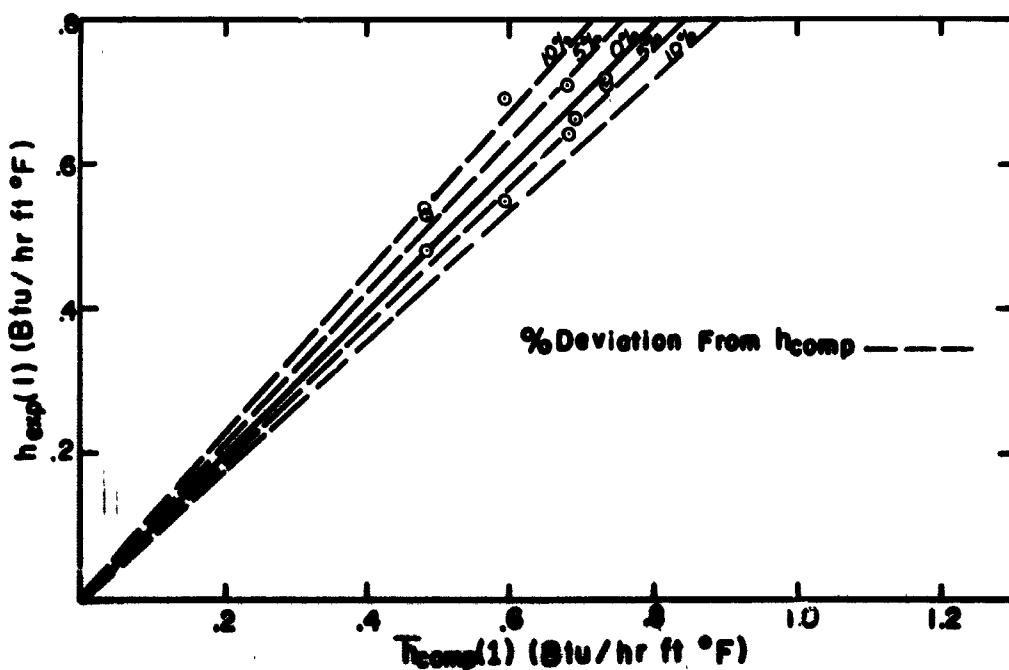

Figure 6.2   Graph of $\bar{h}_{exp}$ vs. $\bar{h}_{comp}$ for Flat Plate

heat losses on the experimentally obtained values of the heat transfer coefficients.

In analyzing the experimental results, lines indicating the per cent deviation were included in the comparison graphs, Figures 6.1 and 6.2, to show the degree of agreement between the experimental and computed values of the average heat transfer coefficients. Figure 6.2 for the flat plate, demonstrates that most experimental values lie within a range of 10% deviation from those of the computed values. From Figure 6.1 it can be seen that the same extent of agreement seems to exist for the cylinder except that the experimental values are consistently higher than those computed. The fact that this can be partly attributed to the difference in the Prandtl number between CO_2 and air, for which the correlations for the cylinder were obtained, suggests that the experimental results for the cylinder are in better agreement with the computed values.

The estimated heat losses in the experiments proved to contain the highest degree of uncertainty. Other pertinent parameters, such as temperature, velocity, and pressure accounted for less than 2% uncertainty. The possible heat loss calculation error approached 10%. This particular uncertainty stemming from the heat losses involves the emissivity value for

VII. CONCLUSIONS AND RECOMMENDATIONS

7.1 Conclusions

1. The experimental results demonstrate clearly that laminar continuum flow conditions existed over the entire range of this investigation. Hence convective heat transfer rates in a Martian atmosphere can be obtained from existing analytic solutions.

2. The maximum error between the measured and calculated values for models tested was of the order of ten per cent. The major portion of this error is attributed to the uncertainties in the estimation of the heat losses.

3. The difference in the Prandtl number of air and carbon dioxide (0.71, 0.77 respectively) does not contribute significantly enough to the results to warrant the use of a specially prepared working fluid.

7.2 Recommendations

1. No further experiments under laminar flow conditions are recommended.

2. Experiments under turbulent flow conditions
with much higher free-stream velocities and
larger test models might be performed, if
so desired.

GENERAL REFERENCES

1. Bird, R. B., Steward, W. E., and Lightfoot, E. N., Transport Phenomena, Wiley, 1960.

2. Eckert, E. R. G. and Drake, R. E., Heat and Mass Transfer, 2nd ed., McGraw Hill, 1959.

3. Kays, W. M., Convective Heat and Mass Transfer, McGraw Hill, 1966.

4. Knudsen, J. G. and Katz, D. L., Fluid Dynamics and Heat Transfer, McGraw Hill, 1958.

5. Rohsenow, W. M. and Choi, H., Heat, Mass and Momentum Transfer, Prentice Hall, 1961.

6. Schlichting, H., Boundary Layer Theory, 6th ed., McGraw Hill, 1968.

7. Schaaf, S. A., Heat Transfer in Rarefied Gases, in Development in Heat Transfer, Rohsenow, ed., MIT Press, 1964, pp. 134-168.

8. Schaaf, S. A. and Chambre, P. L., Flow of Rarefied Gases, Section H of Fundamentals of Gas Dynamics, Emmons ed., Vol III, Princeton Series on High Speed Aerodynamics and Jet Propulsion, Princeton U. Press, 1958, pp. 687-739.

9. Westenberg, A. A., A Critical Survey of the Major Methods for Measuring and Calculating Dilute Gas Transport Properties, in Advances in Heat Transfer, Vol. 3, Academic Press, 1966, pp. 253-302.